The Role of e-Antigen in Hepatitis B Virus Infection

April Leigh Saul

Thesis submitted to the Faculty of the
Virginia Polytechnic Institute and State University
in partial fulfillment of the requirements for the degree of

Master of Science
in
Mathematics

Stanca Ciupe, Chair
Matthias Chung
Lizette Zietsman

May 6, 2015
Blacksburg, Virginia

Keywords: Hepatitis B Virus, e-Antigen

The Role of e-Antigen in Hepatitis B Virus Infection

April Leigh Saul

(ABSTRACT)

Mathematical modeling of biological systems has improved the knowledge of scientists for many years. In virology, particularly in the study of hepatitis B virus, mathematical models were used to explain interactions between hepatitis B virus and the human host in the absence and presence of interventions such as drug therapy and vaccines. This thesis seeks to explain the role of e-Antigen, a particle produced by hepatitis B virus, in the pathogenesis of hepatitis B infection. To accomplish this goal, I will provide biological background as well as previous modeling work on the role of e-Antigen in hepatitis B virus infection, before finally developing a new model adapted specifically for connecting hepatitis B progression with e-Antigen and drug therapy. I will analyze the model both analytically and numerically, fit it to virus data from humans chronically infected with hepatitis B that undergo drug therapy, and draw conclusions about the relation between drugs, immune activation, and loss of e-Antigen.

Acknowledgments

I would like to extend a special thank you to my research advisor, Dr. Stanca Ciupe, for sharing with me her knowledge of mathematical modeling as well as her guidance and support throughout this thesis project. I would also like to thank Dr. Matthias Chung and Dr. Lizette Zietsman for their support of my research.

Further thanks to my parents, Rob and Kay Saul, and grandparents, Lee and Kathern Anthony and Elayne Saul, for their encouragement and financial support.

Contents

List of Figures

List of Tables

Chapter 1

Biology Background

1.1 Hepatitis B Virus (HBV)

Since this thesis seeks to explain a biological phenomenon, a brief explanation of the biology involved must accompany the mathematical model. The biological background will provide vital information about the key components that the thesis will model as well as provide context as to why the hepatitis B virus merits study.

1.1.1 Virus

Hepatitis B virus (HBV) is a double-stranded DNA virus with a circular structure that targets hepatocytes, the type of cell comprising the majority (70%) of the liver [24, 26]. HBV belongs in the family of viruses known as Hepadnaviridae [24]. The small size of the HBV genome allows for the creation of only a few types of proteins [24]. The five proteins that are produced by the HBV genome are the HBV surface antigen, the X-Antigen, a polymerase, the Hepatits B core antigen and the Hepatits B precore Antigen which is also known as the Hepatits B e-Antigen [26]. This last protein will be the focus of our research.

Transmission of HBV occurs due to contact with an infected individual's bodily fluids and the leading cause of adult infections are due to sexual transmission [27]. For regions where HBV is prominent, the most common form of transmission is perinatal transmission, which is the spread of the disease from mother to child during birth [27]. Estimates show that approximately two billion people have been infected with HBV and there are between ten and thirty million new cases every year [12].

There are two types of hepatits B infections: a transient infection and a chronic infection [24]. The immune system of a healthy adult can clear an HBV infection effectively enough that more than ninety-five percent of infections in healthy adults are transient infections [27]. A patient with a transient infection will experience severe illness which will

result in fatality from acute liver failure in 0.5% of cases [24]. Children and infants have a far greater risk of developing a chronic infection with an estimated thirty to fifty percent of infected children and eighty to ninety percent of infected infants contracting a chronic infection [27]. Chronic infections lead to liver disease, cirrhosis of the liver, liver cancer, and death [27]. In regions with high infection numbers, the most common transmission of HBV occurs in a perinatal or childhood infection, hence will likely become chronic [27]. Perinatal infections occur with a greater than ninety percent probability when the mother has an Hepatitis B e-Antigen positive chronic infection [26]. For patients with chronic infections, an infection lasting over six months, 25% will develop liver cancer, leading to a worldwide death toll of over one million people per year [24]. In the United States, on average, one health care provider dies every day from HBV infection which makes the disease a risk to the medical community [12]. Hepatitis B is even classified as the tenth leading cause of death in the world [26]. Individuals with a chronic infection usually are lifelong carriers of the disease [24]. Currently approximately 350 million carriers of HBV live throughout the world with 75% living in southwest Asia [2, 24].

The properties of the liver itself provide an environment advantageous for a chronic infection [24]. Since the hepatocytes regularly enter the bloodstream as blood flows through the lobules of the liver, the infection spreads so that the entire population of hepatocytes becomes infected [24]. Also, the long half-life of the hepatocyte cells (6 to 12 months) will increase the chances of a chronic infection if a strong immune response does not clear the virus in time [24]. The immune response to both acute and chronic infections can cause cirrhosis of the liver as the immune system destroys a large percent of the hepatocytes which are then replaced with scar tissue [24]. Chronic infections result when the immune response is either tolerant or is not strong enough to clear the virus [24]. The immune response in the form of cytotoxic T-cells, in particular, must be strong in order for the virus to be cleared [14]. Therefore very young children and adults with a compromised immune system are likely to develop a chronic infection after contracting HBV [24]. The majority of individuals infected with HBV while very young, became carriers and did not receive treatment, do not suffer from either liver disease [2].However, following an asymptomatic period lasting between twenty and thirty years immune activation occurs spontaneously and leads to liver cirrhosis and liver cancer [26].

Although the hepatocytes have half-lives between six and twelve months under normal circumstances, when the conditions of the liver require the liver to re-generate, the hepatocytes can begin to divide at an accelerated rate [24]. This property comes into play during the immune response to cells infected with HBV [24]. As the immune system kills the hepatocytes which are infected with HBV, liver damage is caused even as the liver cells increase their half-lives to compensate [26].

A vaccine for HBV has existed since 1982 [27]. The vaccine has an efficiency of 95% and is very safe [27]. Over one billion people have received the HBV vaccination worldwide and the percentage of chronically infected children has dropped significantly [27].

1.1.2 Liver Regeneration

Liver regeneration is noticed during hepatitis B infection [6]. Studies indicate that no one gene is irreplaceable in liver regeneration and liver regeneration is caused by a very complex pattern of biological networks [10]. Liver regeneration is triggered by the innate immune system which prompts hepatocytes to recognize the growth factors necessary for cell cycle to begin [10]. The process replaces lost liver mass [10].

1.1.3 e-Antigen

One of the proteins produced by the HBV genome is the Hepatitis e-Antigen (HBeAg) [24]. HBeAg is not needed for the replication of the hepatitis B virus [24]. HBeAg first appears druing the beginning phases of HBV infection [19]. Presence of HBeAg in an infected individual implies that the virus is replicating quickly and the person is highly contagious [27]. However, an individual whose blood test shows a negative result for the presence of HBeAg is not guaranteed to have inactive replication of virions [11]. The creation of HBeAg by the virions triggers the immune system to create Hepatitis B e-Antibodies (HBeAb) [11]. HBeAb can be found in the blood samples of individuals who have either recently recovered from a transient infection or those who are chronically infected [11]. HBeAg is the mechanism responsible for the lack of liver disease occurrences in chronic patients since it inhibits the function of T-cells [4]. HBeAg is considered a tolerogen since it leads to immune tolerance and is especially effective in insuring that prenatal infections are not cleared by the host [26]. HBeAg plays an important role in whether or not an HBV infection will become chronic [26].

HBeAg serocoversion is an important event in the progression of the HBV infection as it indicates the infection has entered the inactive phase [2]. One possible reason for the HBeAg serocoversion is the creation of HBeAb [4]. Another possible explanation is that the HBV genome mutates and creates a population of virions that mainly are HBeAg-negative [4, 30]. The most common type of mutation leading to HBeAg-negative virus is the precore G1896A mutation which changes the DNA secquence to include a stop codon where HBeAg synthesis would occur [30]. During the inactive phase of HBV infection, little liver damage occurs [4]. For approximately $20 - 30\%$ of infected individuals, the infection will re-activate at some point in the future, though re-activation after more than ten years is very unlikely [2]. If re-activation does occur, severe liver damage will follow [4]. The age at which a patient experiences HBeAg serocoversion is related to whether or not re-activation of the virus will take place [4].

Although loss of HBeAg is associated with liver disease, a positive disease outcome is highly correlated to the age of HBeAg seroconversion [3]. Seroconversion occuring between the ages of fifteen and thirty-five is considered the typical time for HBeAg seroconversion among chronically infected patients who were infected at a young age [3]. A very small percent of such individuals, 1.1% for ages less than thirty and 4.4% for ages between thirty

and thirty-nine, will develop liver cirrhosis [3]. However, for patients with delayed seroconversion the odds of developing liver cirrhosis are much higher: 27.3% for ages between forty and forty-nine and 33.3% for patients who undergo seroconversion above the age of fifty [3]. Therefore it is important to understand why seroconversion occurs and whether we can speed up its occurrence.

1.1.4 Immune Response

Two types of immune responses against HBV have been reported [6]. The non-cytolytic response is the response in which infected cells are cured and a cytolytic response is where the immune system kills infected cells [6]. A non-cytolytic response alone will not produce viral clearance, the cytolytic immune response is what is vital for the clearance of HBV [6]. The first immune reaction to HBV is not specific to the virus and incorporates immune cells such as Kupffer cells and the interferon system [15]. The T-cells play the main role in clearing HBV [15]. T-cells are distinguished by their T-cell receptors which allow them to recognize specific molecules that signal them to destroy infected cells [15]. Not only do T-cells directly kill infected cells, they also create toxins which will kill infected cells [15]. The liver damage associated with HBV is caused by the immune response as the immune system destroys the infected cells [15].

1.1.5 Treatment

Treatment options exist for chronic infections, however nothing is known for transient infections other than providing for the comfort and nutritional balance of the patient [27]. Drugs exist for the treatment of a chronic infection which will slow the rate of cirrhosis as well as decrease the risk for liver cancer, hence increase the survival time of the infected individual [27]. The treatment of HBV generally produces a decay in the viral load which is biphasic or triphasic: a high rate of virus decline then a slower rate preceding due to the death of infected cells with a possible plateau phase between the fast and slow decay rates [17]. Problems do exist with the therapy options [26]. One problem is that the virus can become resistant to the treatment through mutations [26]. Another problem is that thirty percent of treated individuals fall into the category of poor responders [26]. In theory, if a drug could regulate the proteins produced by HBV that lead to immune tolerance, that drug could produce a better outcome in a higher percentage of patients [26].

Chronic HBV patients currently have two types of drugs available to treat the virus [26]. One category of drug therapy, the antiviral agents, work by decreasing the reproduction rate of the virions [26]. Antiviral agents require long term therapy and they are costly [26]. An even greater concern is they present a high risk of creating virus mutations which are resistant to the therapy and could lead to a virus strain against which the HBV

vaccine would prove ineffective [26]. The other treatment options are immune-based therapies which increase the immune systems effectiveness in fighting the virus [26]. Like the antiviral agents, immune-based therapies have associated problems [26]. The immune-based therapies are costly and have many side effects [26]. Immune-based therapies also only seem to be effective for patients with low HBeAg levels [26]. In general, immune-based therapies are not effective for sixty to seventy percent of patients [26]. The drug therapy options also cannot be administered over a long period of time [26]. Lamivudine therapy has been found to lead to drug resistance after six months of treatment [16]. HBeAg-positive patients have a much higher probablity of becoming drug resistant than HBeAg-negative patients [16].

A new therapy option targets HBsAg to eliminate the antigen [26]. The therapy option is called immunoglobulin therapy and doctors can use it with the immune-based therapies to improve their success rate [26]. Biologists hope to develop a similar therapy option that can eliminate some of the HBeAg in the blood stream which would logically lead to better therapy response [26].

1.2 Statistical Findings

Many mathematicians have sought to explain aspects of HBV through statistical analysis. One statistical study looked at the virus levels of people with chronic HBV who had undergone spontaneous HBeAg seroconversion [2]. The results showed that all the patients studied showed no signs that the disease had progressed since HBeAg seroconversion and the levels of virus in patients did not seem to be effected by gender or the genotype of the HBV [2]. Statistics has also been applied to analyzing the diversity of HBV genotypes in individuals who experience HBeAg seroconversion and those that do not [29]. The results indicate that before seroconversion, the two groups show no statistical difference in the diversity of the HBV genomes, however, after seroconversion, those patients showed statistically significant greater diversity in the HBV genomes [29].

1.3 Mathematical Models of Hepatitis B Infection

Mathematical models have been used for many years to explain various biological process and to make predictions about the behavior of the modeled variables. Daniel Bernoulli was the first to develop a mathematical model to study an infectious disease, in 1760, focusing on smallpox infection [28]. Since then mathematicians have modeled many other biological processes, and in the 1980s, work began with modeling in-host infections of HIV, HCV, and HBV [28]. Models can explain virus dynamics both within a population as well as inside a host [28]. Scientists' understanding of the diseases induced by viruses such as HBV have been greatly aided by mathematical analysis of the changes in virus level over time in

the human host [17]. Analysis of the changes of the virus levels during antiviral therapy has also provided critical information about the dynamics of the virus and efficacy of the drugs [17]. Most important models have allowed researchers to make predictions and test hypotheses [28].

The first model of HBV infection was created by Nowak et al. in 1995 [21]. The model uses ordinary differential equations that relate the change in target cells, infected cells and virions in the simplest form possible [21]. Assume x represents the target hepatocytes, y indicates the infected and v represents hepatitis B virus [21], then the equations are:

$$\frac{dx}{dt} = \lambda - dx - bvx, \tag{1.1}$$
$$\frac{dy}{dt} = bvx - ay, \tag{1.2}$$
$$\frac{dv}{dt} = ky - uv, \tag{1.3}$$

where, λ is the production rate of the target cells, b is the rate that cells are infected through contact with the virus, d is the death rate of uninfected cells and a is the death rate of infected cells [21]. The infected cells produce k virions and the virions are cleared at rate u [21]. The system of equations will cause the populations to reach the steady state of chronic infection when

$$R_0 = \frac{\lambda bk}{adu} > 1.$$

The R_0, called the basic reproductive number, represents the number of secondary infections induced by one infected cell in a naive population [1]. The model indicates that if drug therapy stops the production of infected cells completely, $k = b = 0$, the virus and infected cell populations will both decay exponentially as expressed by:

$$v(t) = v_0 e^{-ut},$$
$$y(t) = y_0 e^{-at}.$$

Tsiang et al. [25] observed that the model proposed by Nowak et al. [21] does not fit data past thirty days of treatment, since Nowark's model cannot reproduce the biphasic decay seen in patient data. Tsiang et al. assumed that during therapy, $b = 0$. However, k is no longer assumed to be zero, allowing for a partial decrease in the production of the virus [25]. The variable ϵ, where $0 \leq \epsilon \leq 1$, was introduced to indicate drug efficacy [25]. The new system is:

$$\frac{dx}{dt} = \lambda - dx - bvx, \tag{1.4}$$
$$\frac{dy}{dt} = bvx - ay, \tag{1.5}$$
$$\frac{dv}{dt} = (1-\epsilon)ky - uv. \tag{1.6}$$

Data fitting showed that ϵ is approximately 0.99, indicating the need of a high drug efficacy [25].

Another modification of model (1.1-1.3) was introduced by Neumann et al. in 1998 [20]. The model includes the effects of drug therapy in both decreasing the number of virions by infected cells with efficacy ν infection of target cells with efficacy ϵ, where $0 \leq \epsilon, \nu \leq 1$ [20]. The system becomes:

$$\frac{dT}{dt} = s - dT - (1-\nu)\beta VT, \tag{1.7}$$

$$\frac{dI}{dt} = (1-\nu)\beta VT - \delta I, \tag{1.8}$$

$$\frac{dV}{dt} = (1-\epsilon)pI - cV. \tag{1.9}$$

The equations were then analyzed for steady states and made predictions on the half-life times of infected cells and virus [20]. Most recent work in HBV uses the following notations: $T = x$, $I = y$, $V = v$, $s = \lambda$, $\beta = b$, $\delta = a$, $p = k$, and $c = u$.

In 2001, Lewin et al. [17] improved model (1.7-1.9) by considering two types of immiune responses: cure of infected cells at rate ρ as seen experimentally [13] and killing of infected cells at rate δ [17]. The system of equations is:

$$\frac{dT}{dt} = s - dT - (1-\eta)\beta VT + \rho I, \tag{1.10}$$

$$\frac{dI}{dt} = (1-\eta)\beta VT - \delta I - \rho I, \tag{1.11}$$

$$\frac{dV}{dt} = (1-\epsilon)pI - cV. \tag{1.12}$$

Another important new concept included is a time delay between the beginning of treatment and when treatment begins to effect the amount of virus [17]. Assuming that target cells are constant at the start of therapy, they solved the now linear system to get the following equation for the virus load [17]:

$$V(t) = \frac{1}{2}\left((1 - \frac{c+\delta-2\epsilon c}{\theta})^{-\lambda_1(t-\tau)} + (1 + \frac{c+\delta-2\epsilon c}{\theta})e^{-\lambda_2(t-\tau)}\right)$$

where $\lambda_{1,2}$ are eigenvalues and $\theta = \sqrt{(c-\delta)^2 + 4(1-\epsilon)(1-\nu)c\delta}$ [17]. They fitted this to data from patients on drug therapy and estimated that the average delay time was 1.6 days [17]. Inclusion of the time delay produces greater accuracy in data fitting than equations without a time delay [17]. The authors also used their model for the calculation of the half-lives of both infected cells and virions [17].

Ribeiro et al. [23] used their model to compare the half-lives of virions and infected cells in two different groups of patients: HBeAg-negative and HBeAg-positive that undergo drug therapy [23]. The analysis showed that half-life of both free virions and infected cells were approximately half as long in the HBeAg-negative infection [23]. This will be relevant

in our own study on the effect of HBeAg during infections.

The most complex model of drug therapy was developed by Dahari et al. [8]. It adds liver regeneration by modeling it using logistic growth in both the uninfected and infected hepatocyte populations. The per capita growth rates are r_T and r_I, and T_{max} is the carrying capacity [8]. The system of equations is:

$$\frac{dT}{dt} = s + r_t T(1 - \frac{T+I}{T_{max}}) - d_T T - (1-\eta)\beta V T + \rho I \tag{1.13}$$

$$\frac{dI}{dt} = (1-\eta)\beta V T + r_I I(1 - \frac{T+I}{T_{max}}) - (\delta + \rho) I \tag{1.14}$$

$$\frac{dV}{dt} = (1-\epsilon) p I - c V \tag{1.15}$$

The model shows complex virus decay patterns based on parameter ϵ_c, called critical drug efficacy [8]. When the total drug efficacy is less than ϵ_c, a rebound is observed in the virus decay plot [8]. For total drug efficacy greater than ϵ_c, either a biphasic or triphasic decay will occur depending on whether the ratio of infected to target cells is greater than or equal to one [8], where

$$\epsilon_c = 1 - \frac{c((\delta+\rho)T_{max} + r_I(T_0 - T_{max}))}{p\beta T_{max} T_0}$$

is the critical drug efficacy, T_0 represents the infection free steady state value of target cells and total drug efficacy is defined as $1 - \epsilon_{tot} = (1-\rho_{max})(1-\epsilon)$ [8].

As explained in the biological introduction, the majority of adult infections result in acute infections and viral clearence. Modeling work on this was done in [5–7, 9]. Moreover, modeling work has been done on determining the dynamics of liver regeneration following transplant [22].

In this thesis we are interested in chronic infections under drug therapy. Therefore, we will build on these models and include the role of HBeAg in inducing chronic infections. Moreover, we will investigate the effect of HBeAg loss on disease pathogenesis.

Chapter 2

The Role of HBeAg During Hepatitis B Prenatal Infection

Little is known about the mechanisms of tollerance/ immune activation. To adress some questions regarding HBeAg persistence, loss, and liver disease, we develop mathematical models that include the dynamics of HBeAg. As discussed in section 1.3, HBeAg is believed to be responsible for inducing immune tolerance in prenatal infections [26]. Moreover, the loss of HBeAg correlates with immune activation and liver disease [3]. We start by reviewing previous work performed by Ciupe et al. [4] which investigated the role of HBeAg during HBV infection. They developed a mathematical model for the role of HBeAg in inducing immune tolerance following HBV prenatal infections. The model also investigates what causes the HBeAg loss and the emergence of immune response leading to probable liver damage.

2.1 Model of HBV Chronic Infection

The model considers the interaction between three populations: V_p, the level of HBeAg-positive virus, e, the level of HBeAg, and T_p, the T-cells specific for hepatitis B. The model assumes that the virus is constant (as in chronic infections) and modeled by a logistic term with per captita rate r_p and carrying capacity K. Virus produces HBeAg at rate π and HBeAg is cleared from the system by immune cells at rate δ. The rate at which the T-cells differentiate after contact with HBeAg at rate α_p. The growth of the T-cell population is limited when HBeAg is present, at rate σ. The lifespan of the T-cell, is $1/d$ days. The virus is cleared from the system at a rate μ_p. The intial conditions for the system are $V_p(0) = 0.3$ per ml, $e(0) = 0.03$ per ml, and $T_p(0) = 10$ per ml.

The interactions are given by the following diagram:

$$\frac{V_p}{dt} = r_p V_p(1 - \frac{V_p}{K}) - \mu_p V_p T_p \tag{2.1}$$

$$\frac{de}{dt} = \pi V_p - \delta e \tag{2.2}$$

$$\frac{dT_p}{dt} = \frac{\alpha_p V_p T_p}{1 + \sigma e} - dT_p \tag{2.3}$$

and are illustrated by:

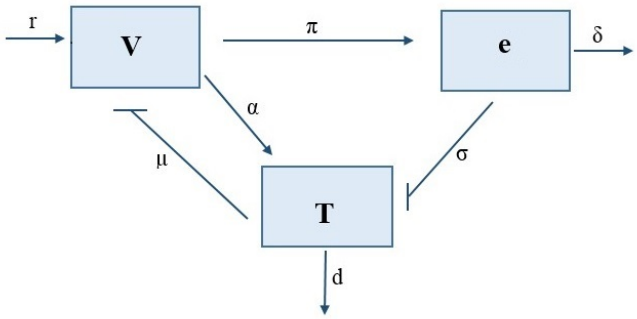

Figure 2.1: The biological picture visually shows the interactions between the variables.

The system has three steady states: $S_0 = (0, 0, 0)$, which represents liver failure, $S_1 = (K, \frac{K\pi}{\delta}, 0)$, which indicates a chronic infection that is immune-tolerant, and $S_2 = (\Omega, \frac{\pi\Omega}{\delta}, \frac{r_p}{\mu_p}(1 - \frac{\Omega}{K}))$ which relates to an immune-competent chronic infection, where

$$\Omega = \frac{d\delta}{\alpha_p\delta - d\sigma\pi}.$$

Through stability analysis one can show that S_1 is asymptotically stable when $0 > \Omega$ or $\Omega > K$ and S_2 is asymptotically stable when $0 < \Omega < K$.

A plot of System (2.1-2.3) can show the effect of a change in α on the steady state. The plot appears as Figure 2.2. When α is small, the immune cells are absent (see first 500 days). When α is increased, T_p reaches a steady state and starts removing virus (last 500 days).

The model provides conditions for which the maximum immune response will occur as well as an idea as to the amount of HBeAg necessary to create T-cell tolerance. The point at which the steady state would switch between S_1 and S_2, marking a loss of tolerance is not dependent on the μ_p which is the rate at which the immune cells eliminate the virus, therefore there is not direct affect from HBeAg on the ability of the T-cells to clear the virus. The immune cells production rate, α_p, however, is affected by the HBeAg, leading to immune tolerance.

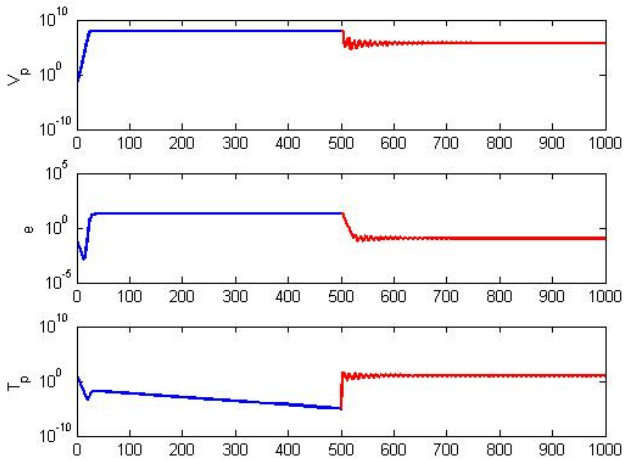

Figure 2.2: The plot shows that a change in α at time $t = 500$ in System (2.1-2.3) will result in immune tolerance transforming into immune activation. The blue line indicates the system in immune tolerance, $\alpha = 10^{-7}$, and the red line shows the system with immune activation due to α increasing to 10^{-6}.

The model can be used to predict the amount of liver damage that occurs after a loss of HBeAg. Assume that at equilibrium, infected cells are proportional to the virus, $H_p^* = \frac{cV_p}{p}$ where c represents the virus clearance rate and p is production rate of the virions. Then let $f = \frac{c}{p}$. The accumulated loss of liver cells can be expressed in the following integral:

$$a_s(\tau) = \int_0^\tau \mu_p f V_p(t) T_p(t) dt.$$

During chronic infections, $T_p \to 0$ and $a_s(\tau)$ is negligible. Next we look at the changes in T_p concentration when HBeAg is lost through either seroconversion, i.e. antibody production or through mutation.

2.1.1 HBeAg Loss Due To Serconversion

When antibodies against HBeAg are produced, HBeAg is lost and the immune cells become functional. This is a spontaneous process observed fifteen to twenty years following infection. The cause is unknown. To model this, Ciupe et al. considered a parameter Ig for the constant HBeAb concentration and ν is the rate at which HBeAb removes HBeAg. The new model is:

$$\frac{V_p}{dt} = r_p V_p(1 - \frac{V_p}{K}) - \mu_p V_p T_p \tag{2.4}$$

$$\frac{de}{dt} = \pi V_p - \delta(1 + \nu Ig)e \tag{2.5}$$

$$\frac{dT_p}{dt} = \frac{\alpha_p V_p T_p}{1 + \sigma e} - dT_p \tag{2.6}$$

and the steady states S_0 and S_1 are the same as in the first model. However, S_2 is the same if $Ig = 0$ and $S_2 = \left(\Omega_{Ig}, \frac{\pi\Omega_{Ig}}{\delta}, \frac{r_p}{\mu_p}(1 - \frac{\Omega_{Ig}}{K})\right)$ if $Ig \neq 0$, where

$$\Omega_{Ig} = \frac{d\delta(1 + \nu Ig)}{\alpha_p\delta(1 + \nu Ig) - d\sigma\pi}.$$

Ciupe et al. set $Ig = 1000$ and plotted variables in (2.1-2.3) for $0 < t < 500$ followed by (2.4-2.6) for $500 < t < 1000$. Figure 2.5 shows the transition between the immune tolerant steady state and the immune activation steady state.

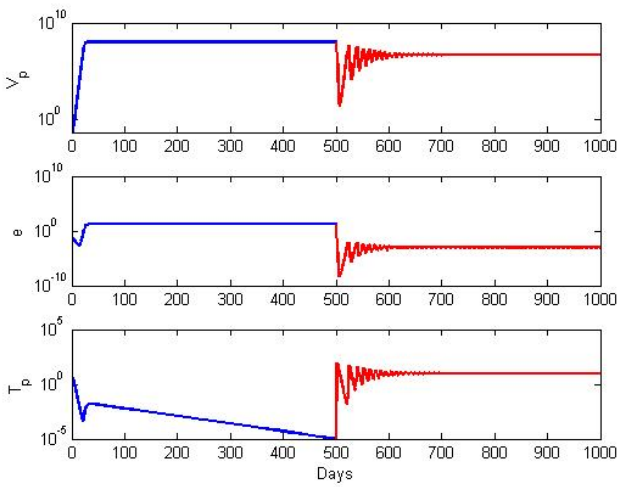

Figure 2.3: Solutions of (2.1-2.3) showing immune tolerance in blue for time $0 < t < 500$ followed by solutions of (2.4-2.6) showing immune activation in red for times $500 < t < 1000$.

A bifurcation diagram which demonstrates the influence of Ig on the V_p and T_p steady states as given for (2.4-2.6) appears in Figure 2.4. For the values of $Ig < Ig_{crit}$, the immune tolerance steady state is stable. The immune activation steady state emerges once $Ig > Ig_{crit}$ where $I_{g_{crit}} = 103.5088$. Another bifurcation diagram, Figure 2.5 shows the influence of I_g on the percent of liver lost cumulatively for time $t = 0$ to $t = \tau = 100$ calculated by $a_s(\tau)$. For $Ig < Ig_{crit}$, liver damage is minimal, however once $Ig > Ig_{crit}$, larger liver damage is observed, reaching a steady state.

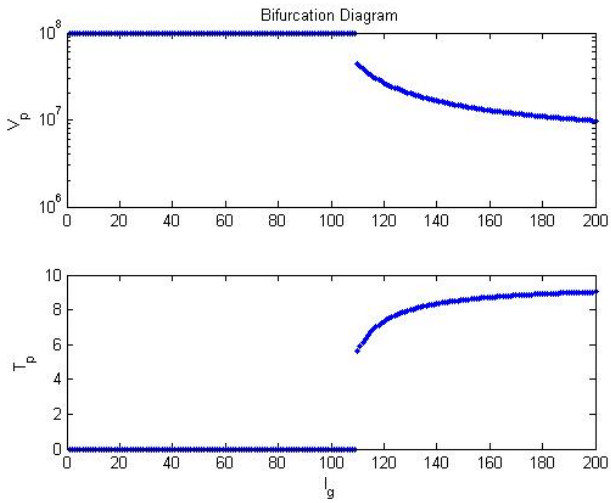

Figure 2.4: The bifurcation diagram for the steady states of V_p and T_p as given by (2.4-2.6) based on changes in Ig where $I_{g_{crit}} = 103.5088$.

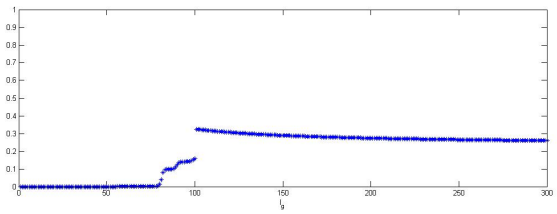

Figure 2.5: The percent of liver lost cumulatively for time $t = 0$ to $t = \tau = 100$ compared to I_g calculated by $a_s(\tau)$.

2.1.2 HBeAg Loss due to Mutations

When HBeAg is lost due to mutations at rate ϕ, HBeAg negative strains, V_n, emerge together with T-responses specific for this new virus strain, T_n. V_n no longer produces HBeAg. Such mutations have been shown to happen biologically [30].

$$\frac{V_p}{dt} = r_p V_p((1-\phi) - \frac{V_p + V_n}{K}) - \mu_p V_p T_p \tag{2.7}$$

$$\frac{V_n}{dt} = r_p V_p(1 - \frac{V_p + V_n}{K}) + r_p \phi V_p - \mu_n V_n T_n \tag{2.8}$$

$$\frac{de}{dt} = \pi V_p - \delta e \tag{2.9}$$

$$\frac{dT_p}{dt} = \frac{\alpha_p V_p T_p}{1 + \sigma e} - dT_p \tag{2.10}$$

$$\frac{dT_n}{dt} = \frac{\alpha_p V_p T_p}{1 + \sigma e} - dT_n \tag{2.11}$$

A diagram for the model is given by Figure 2.6.

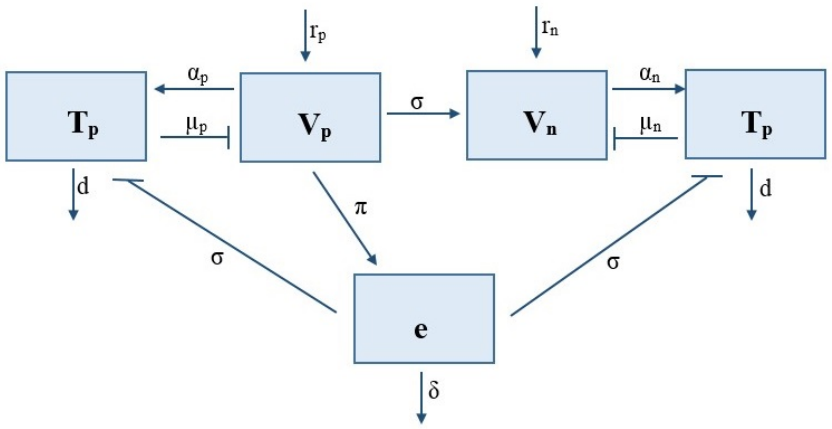

Figure 2.6: The biological picture demonstrates the interactions between the variables.

This new model has four different steady states that represent the various forms of immune activation, with the most relevant being the one in which V_p is completely lost.

Graphs can visually demonstrate the differences in the transition between immune tolerance and immune activation with a moderate degree of mutation versus a large degree of mutation. A moderate mutation rate only result in a loss of HBeAg and large mutation rate will result in clearence of HBeAg. Figure 2.7 shows a moderate mutation rate and Figure 2.8 shows the larger mutation rate.

One can compute the amount of liver damage resulting from immune activations as:

$$a_{sm}(\tau) = \int_0^\tau (\mu_p f V_p(t) T_p(t) + \mu_n f V_n(t) T_n(t)) dt, \text{ for small mutations and}$$

$$a_{hm}(\tau) = \int_0^\tau \mu_n f V_n(t) T_n(t) dt = \tau f r_p \frac{d}{\alpha_n}\left(1 - \frac{d}{K\alpha_n}\right), \text{ for big mutations.}$$

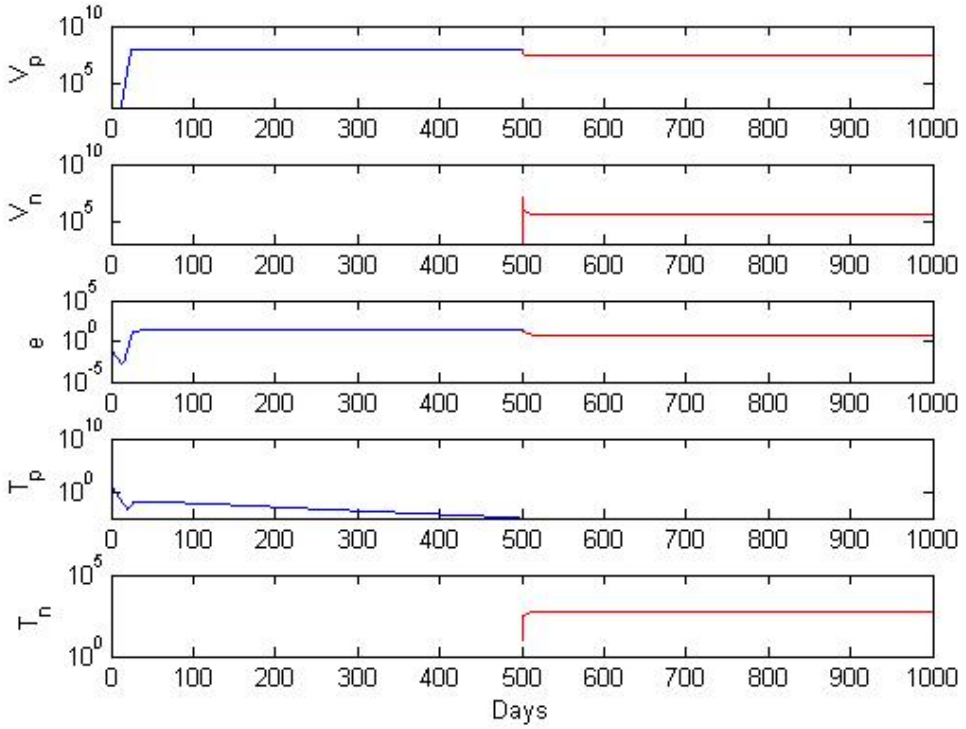

Figure 2.7: The plot shows System (2.1-2.3) in the immune tolerance steady state in blue followed by System (2.7-2.11) depicted in red, indicating immune activation begining as a result of a moderate degree of HBV mutation, $\phi = 0.7$.

Bifurcation diagrams showing $a_{sm}(\tau)$ and $a_{hm}(\tau)$ versus ϕ for $\tau = 100$ are given in Figure 2.9. The figure shows that the liver damage is minimal when the mutation rate ϕ is high. Moreover, they show killing of the liver as 1.8 times at $t = 100$ days post immune activation for $\phi = 0.85$. Liver loss, however is compensated by the increase of liver cells due to division. Mathematically, this is given by:

$$p(\tau) = \int_0^\tau (r_p H_p^*(t) + r_p H_n^*)\left(1 - \frac{H_p^* + H_n^*(t)}{L}\right) dt.$$

The overall liver loss $p(\tau) - a(\tau)$ is negligible for all mutation and serconversion induced immune activation. However, liver turnover is detrimental to the patient as it induces mutations and leads to liver cancer.

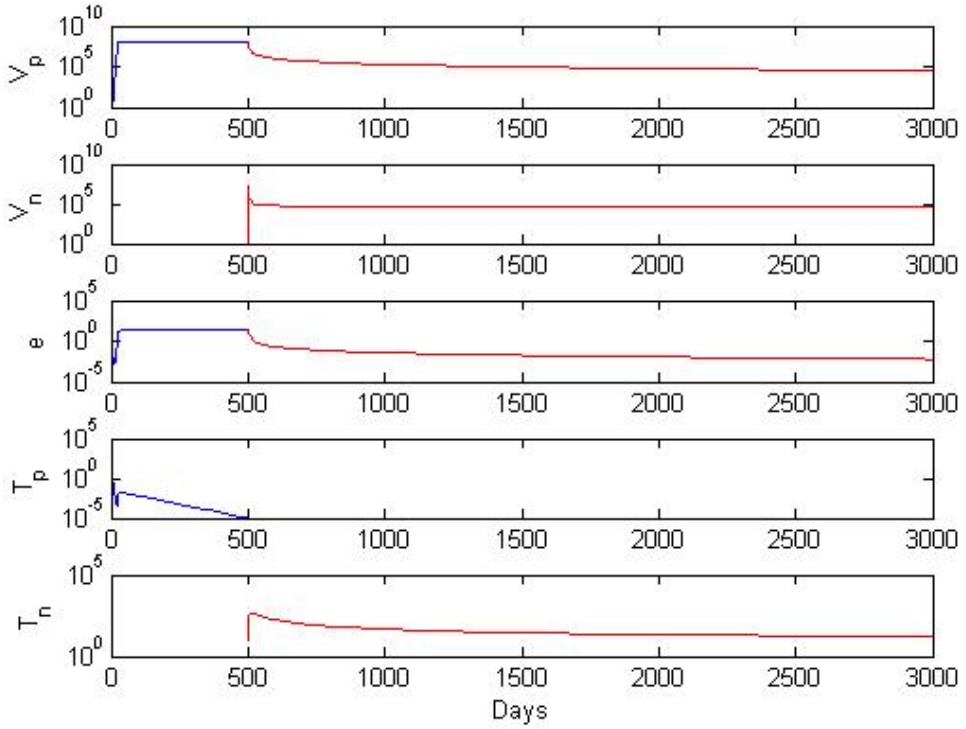

Figure 2.8: The plot shows System (2.1-2.3) in the immune tolerance steady state in blue followed by System (2.7-2.11) depicted in red, indicating immune activation begining as a result of a large degree of HBV mutation, $\phi = 0.9997$.

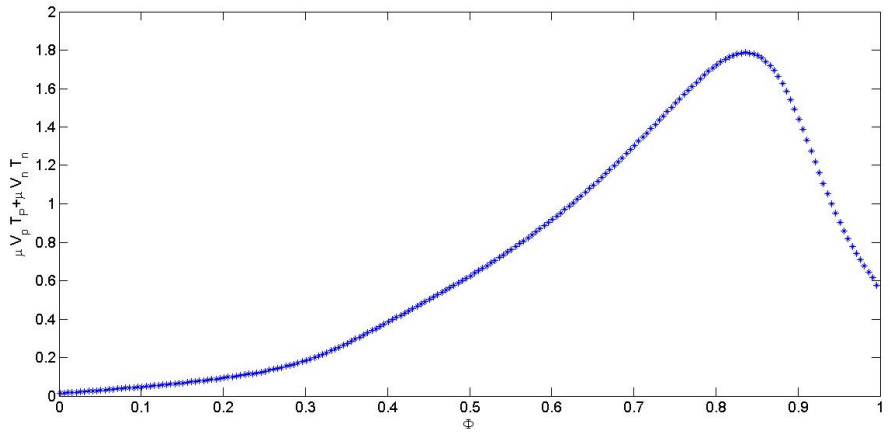

Figure 2.9: The plot shows the influence of ϕ on the cumulative liver percentage loss due to mutations for time $t = 0$ to $t = \tau = 100$.

Chapter 3

Model of e-Antigen Effect in HBV Infection Under Drug Therapy

3.1 Motivation

The results in [4] caught the attention of hepatologists from Loyola Medical School, who want to understand why and when seroconversion occurs. Dr. Harel Dahari and Dr. Scott Cotler shared with us historical data of patients from the Chicago area who were infected at birth and who were sampled at ages twenty-six to fifty-five post infection and around HBeAg seroconversion [18]. All of the patients, however, were undergoing drug therapy at the time data was collected. To model this, we need to modify model (2.1-2.3) to account for target and infected hepatocytes and the effect of drugs on their dynamics.

3.2 Model of HBV Infection without Drug Therapy

We expand model (2.1-2.3) to account for uninfected and infected liver cells. We model the intraction between target cells, T, infected cells, I, virus, V, e-Antigen, e, and effector cells, E. Target cells are produced at per capita rate r. We assume that the growth is modeled by a logistic term with carrying capacity T_m. Cells become infected at rate k and die at rate δ_I (due to viral toxicity) and are killed by effector cells at a rate μ. Infected cells produce p virions which are cleared at rate c. Virus produce e-Antigen at a rate π and the e-Antigen is cleared at a rate δ_e. Effector cells expand in the presence of infected cells at rate α. The expansion is limited by the presence of e-Antigen at rate σ. Finally, effector cells die at rate d_E. The equations representing the interactions are:

$$\frac{dT}{dt} = rT\left(1 - \frac{T+I}{T_m}\right) - kTV, \tag{3.1}$$

$$\frac{dI}{dt} = kTV - \delta_I I - \mu IE, \tag{3.2}$$

$$\frac{dV}{dt} = pI - cV, \tag{3.3}$$

$$\frac{de}{dt} = \pi V - \delta_e e, \tag{3.4}$$

$$\frac{dE}{dt} = \frac{\alpha IE}{1+\sigma e} - d_E E. \tag{3.5}$$

and the initial conditions are: $T(0) = T_0$ cells/mL, $I(0) = I_0$ cells/mL, $V(0) = V_0$ virus/mL, $e(0) = e_0$ per mL, and $E(0) = E_0$ cells/mL.

The system can also be represented visually by diagram 3.1.

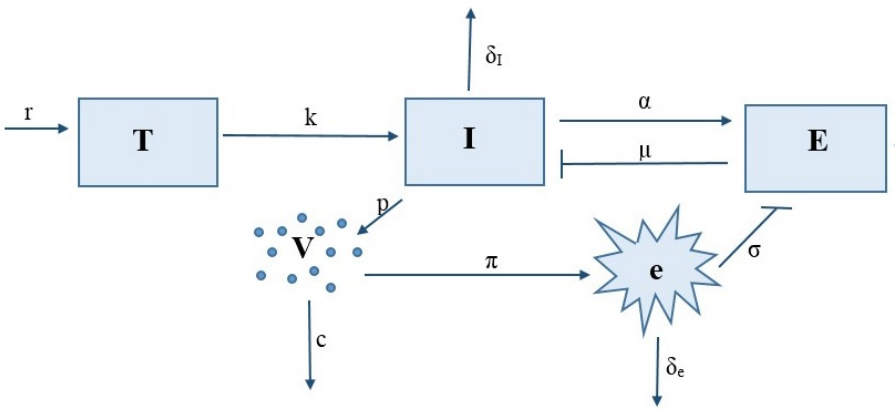

Figure 3.1: The biological picture demonstrates the interactions between the variables.

3.2.1 Stablity Analysis

System (3.1-3.5) has three biologically significant steady states:

$$S_0 = (T_m, 0, 0, 0, 0),$$

which represents the no infection steady state. S_0 always exists. The second steady state,

$$S_1 = (T_1, I_1, V_1, e_1, 0),$$

is a chronic infection steady state in the absence of effector cells and

$$
\begin{aligned}
T_1 &= \frac{c\delta_I}{kp},\\
I_1 &= \frac{cr(kpT_m - c\delta_I)}{pk(cr + kpT_m)},\\
V_1 &= \frac{r(kpT_m - c\delta_I)}{k(cr + kpT_m)},\\
e_1 &= \frac{\pi r(kpT_m - c\delta_I)}{\delta_e k(cr + kpT_m)}.
\end{aligned}
$$

S_1 exists when $R_{01} = \frac{kpT_m}{c\delta_I} > 1$.

The third steady state is:

$$S_2 = (T_2, I_2, V_2, e_2, E_2)$$

which is a chronic infection steady state in the presence of effector cells, where:

$$
\begin{aligned}
T_2 &= T_m - \frac{d_E\delta_e(rc + kpT_m)}{r(c\delta_e\alpha - d_E\pi\sigma)},\\
I_2 &= \frac{cd_E\delta_e}{c\delta_e\alpha - d_Ep\pi\sigma},\\
V_2 &= \frac{d_E\delta_e p}{c\delta_e\alpha - d_Ep\pi\sigma},\\
e_2 &= \frac{d_Ep\pi}{c\delta_e\alpha - d_Ep\pi\sigma},\\
E_2 &= \frac{kpT_m - c\delta_I}{c\mu} - \frac{kpd_E\delta_e(rc + kpT_m)}{rc\mu(c\delta_e\alpha - d_Ep\pi\sigma)}.
\end{aligned}
$$

S_2 exists when

$$
\begin{aligned}
\sigma &< \frac{c\delta_e\alpha}{d_Ep\pi},\\
rT_m(c\delta_e\alpha - d_E\pi\sigma) &> d_E\delta_e(rc + kpT_m), \text{ and}\\
R_{02} &= \frac{kpd_E\delta_e(rc + kpT_m)}{rc\delta_I(c\delta_e\alpha - d_E\pi\sigma)} > 1.
\end{aligned}
$$

We want to study the local stability of system (3.1-3.5). The Jacobian associated to it is

$$J = \begin{pmatrix} r(1-\frac{T+I}{T_m}) - \frac{rT}{T_m} - kV - \lambda & \frac{-rt}{t_m} & -kT & 0 & 0 \\ kV & -\delta_I - \mu E - \lambda & kT & 0 & I\mu \\ 0 & p & -c-\lambda & 0 & 0 \\ 0 & 0 & \pi & -\delta_e - \lambda & 0 \\ 0 & \frac{\alpha E}{1+e\sigma} & 0 & \frac{-\alpha E I \sigma}{(1+e\sigma)^2} & \frac{\alpha I}{1+e\sigma} - d_E - \lambda \end{pmatrix}$$

Proposition 1 Steady State S_0 is locally asymptotically stable when

$$R_{01} < 1,$$

and unstable otherwise.

Proof The characteristic equation for S_0 is:

$$(-d-\lambda)(-\delta_e-\lambda)(-r-\lambda)(\lambda^2 + (\delta_I + c)\lambda + (c\delta_I - kpT_m)) = 0,$$

and the corresponding eigenvalues are

$$\begin{aligned} \lambda_1 &= -\delta_e < 0, \\ \lambda_2 &= -d_E < 0, \\ \lambda_3 &= -r, < 0, \\ \lambda_4 &= \frac{-c - \delta_I + \sqrt{c^2 - 2c\delta_I\delta_I^2 + 4kpT_m}}{2}, \\ \lambda_5 &= \frac{-c - \delta_I - \sqrt{c^2 - 2c\delta_I\delta_I^2 + 4kpT_m}}{2} < 0. \end{aligned}$$

$\lambda_4 < 0$ when $R_{01} < 1$. Therefore S_0 is locally asymptotically stable when $R_{01} < 1$.

Proposition 2

S_1 is locally asymptotically stable when

$$1 < R_{01} < R_{01}^*$$

and

$$\sigma > \frac{\alpha c \delta_e}{p\pi d_E} - \frac{k\delta_e}{\pi r}\frac{cr + kt_m p}{kT_m p - c\delta_I}.$$

Proof The characteristic equation for S_1 is:

$$\left(\frac{\alpha c\delta_e r(kpT_m - c\delta_I)}{p\Big(\delta_e k(cr + kT_m) + \pi r(kpT_m - c\delta_I)\sigma\Big)} - d_E - \lambda\right)(-\delta_e - \lambda)(\lambda^3 + A_1\lambda^2 + A_2\lambda + A_3) = 0,$$

where

$$\begin{aligned} A_1 &= c + \delta_I + \frac{cr\delta_I}{kpT_m} \\ A_2 &= \frac{rc^2\delta_I}{kpT_m} + \frac{r\delta_I c(r+\delta_I)}{rc+kpT_m} \\ A_3 &= \frac{rc\delta_I}{kpT_m}(kpT_m - c\delta_I) \end{aligned}$$

In order for S_1 to be stable,

$$\lambda_1 = \frac{\alpha c\delta_e r(kpT_m - c\delta_I)}{p(\delta_e k(cr+kT_m) + \pi r(kpT_m - c\delta_I)\sigma)} - d_E$$

must be negative. Therefore, if the steady state is stable then

$$\sigma > \frac{\alpha c\delta_e}{p\pi d_E} - \frac{k\delta_e}{\pi r}\frac{cr+kT_m p}{kT_m p - c\delta_I}$$

The second eigenvalue, $\lambda_2 = -d_E$ is always negative.

Finally, by Routh Hurwitz condition, we need $A_1 > 0$, $A_3 > 0$, and $A_1A_2 - A_3 > 0$ for stability. They hold when $R_{01} > 1$ and $R_{01}^* > R_{01} > 1$ where

$$R_{01}^* = \frac{c^2 + 3c\delta_I + \delta_I^2 + cr + \delta_I r}{cr + kpT_m} + \frac{c^3\delta_I r^2}{k^2p^2T_m^2(cr+kpT_m)} + \frac{r(c^3 + 3c^2\delta_I + c\delta_I^2 + c\delta_I r)}{kpT_m(cr+kpT_m)}.$$

The stability of S_2 tedious and we will present only numerical results.

3.2.2 Numerical Results

The different steady states of system (3.1-3.5) can be reached with parameter sets in which only σ changes. σ represents the effect of a change in the rate at which HBeAg limits the expansion of the effector cells. Figure 3.2 shows the system reaching steady state S_1 which occurs when σ is high ($\sigma = 2.1$ cells per mL $\times$ day.) so the immune system does not expand in the presence of HBV (E goes to zero). That leads a low steady state value for the target cells and a high steady state value for the infected cells. When $\sigma = 2.1$, $T_1 = 2.9 \times 10^5$ cells per mL and $I_1 = 5.0 \times 10^6$ cells per mL. For a low value of σ ($\sigma = 0.0021$ cells per mL $\times$ day.) the immune system can recognize the presence of HBV and therefore create the needed effector cells, the state which steady state S_2 represents. Figure 3.3 shows the system

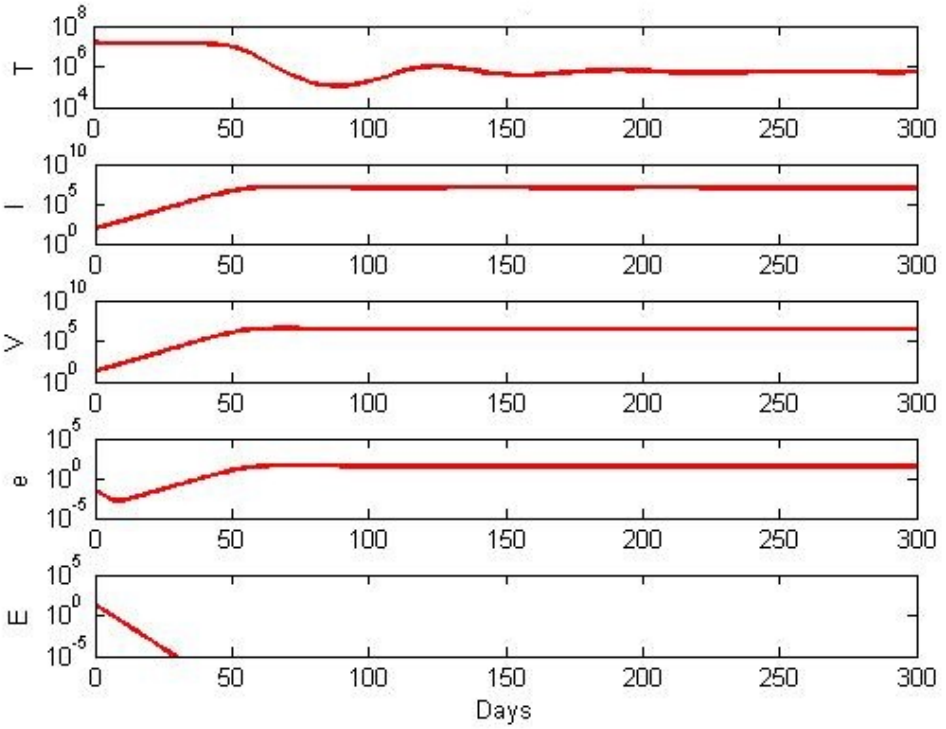

Figure 3.2: The plot of all five variables over time reaching steady state S_1 with $\sigma = 2.1$ cells per mL $\times$ day.

reaching steady state S_2 with $\sigma = 0.0021$. The new steady state values become $T_2 = 5.0 \times 10^6$ cells per mL, a 1065.5% difference, and $I_2 = 6.5 \times 10^6$, a 34.3% difference.

As in model (2.1-2.3) we want to see when the tolerance is lost, by looking for loss of HBeAg or the HBeAg effect, σ.

3.3 Model with constant Effector Cell Growth s_E

Due to numerical difficulties induced by low values of effector cells, we changed model (3.1-3.5) to account for a baseline of effector cells in the body. We model this by assuming that there is a constant influx of effector cells s_E. The model becomes:

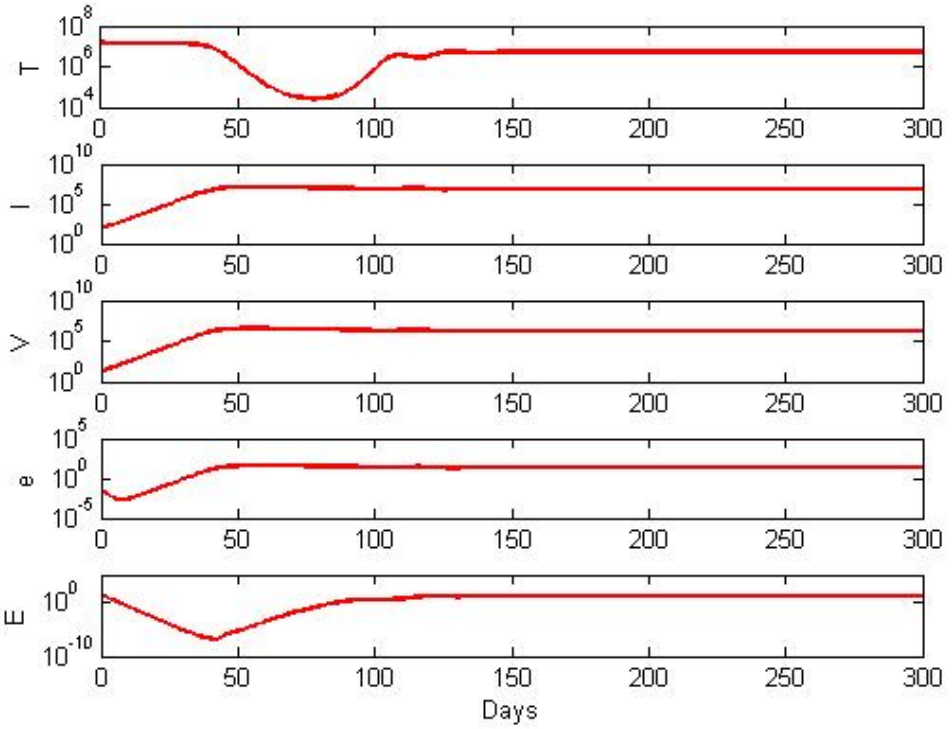

Figure 3.3: The plot of all five variables over time reaching steady state S_2 with $\sigma = 0.0021$ cells per mL $\times$ day.

$$\frac{dT}{dt} = rT\left(1 - \frac{T+I}{T_m}\right) - kTV, \tag{3.6}$$

$$\frac{dI}{dt} = kTV - \delta_I I - \mu IE, \tag{3.7}$$

$$\frac{dV}{dt} = pI - cV, \tag{3.8}$$

$$\frac{de}{dt} = \pi V - \delta_e e, \tag{3.9}$$

$$\frac{dE}{dt} = s_E + \frac{\alpha IE}{1+\sigma e} - d_E E. \tag{3.10}$$

3.3.1 Stablity Analysis

The behavior of system (3.6-3.10) is similar to that of (3.1-3.5). Briefly, it also has three biologically significant steady states:

$$S_0 = (T_m, 0, 0, 0, \frac{s_E}{d_E})$$

which is the no infection steady state. S_0 always exists. The second steady state,

$$S_1 = (T_1, I_1, V_1, e_1, E_1),$$

is a chronic infection steady state where effector cells are functional, where

$$\begin{aligned}
T_1 &= \frac{cr\Big(\delta_e\Big(c\delta_I\alpha - kp(d_E - T_m\alpha)\Big) - \sigma p\pi(d_E\delta_I + \mu s_E)\Big) - d_E kp^2 T_m(\delta_e k + \pi r\sigma) + \sqrt{\Omega}}{2kpr(d_E p\pi\sigma - c\delta_e\alpha)},\\
I_1 &= \frac{c\Bigg(cr\Big(\delta_e\Big(c\delta_I\alpha - kp(d_E + T_m\alpha)\Big) - \sigma p\pi(d_E\delta_I + \mu s_E)\Big) + d_E kp^2 T_m(\delta_e k - \pi r\sigma) - \sqrt{\Omega}\Bigg)}{2kp(d_E p\pi\sigma - c\delta_e\alpha)(cr + kpT_m)},\\
V_1 &= \frac{cr\Big(\delta_e\Big(c\delta_I\alpha - kp(d_E + T_m\alpha)\Big) - \sigma p\pi(d_E\delta_I + \mu s_E)\Big) + d_E kp^2 T_m(\delta_e k - \pi r\sigma) - \sqrt{\Omega}}{2k(d_E p\pi\sigma - c\delta_e\alpha)(cr + kpT_m)},\\
e_1 &= \frac{\pi\Bigg(cr\Big(\delta_e\Big(c\delta_I\alpha - kp(d_E + T_m\alpha)\Big) - \sigma p\pi(d_E\delta_I + \mu s_E)\Big) + d_E kp^2 T_m(\delta_e k - \pi r\sigma) - \sqrt{\Omega}\Bigg)}{2k\delta_e(d_E p\pi\sigma - c\delta_e\alpha)(cr + kpT_m)},\\
E_1 &= \frac{cr\Big(\delta_e\Big(c\delta_I\alpha + kp(d_E - T_m\alpha)\Big) - \sigma p\pi(d_E\delta_I - \mu s_E)\Big) + d_E kp^2 T_m(\delta_e k + \pi r\sigma) + \sqrt{\Omega}}{2c\mu r(d_E p\pi\sigma - c\delta_e\alpha)}.
\end{aligned}$$

and

$$\begin{aligned}
\Omega &= 4c\mu prs_E(c\delta_e\alpha + dp\pi\sigma)(cr(\delta_e k + \delta_I\pi\sigma) + kpT_m(\delta_e k + \pi r\sigma)) + (c^2\delta_e\delta_I r\alpha + d_E kp^2 T_m(\delta_e k + \pi r\sigma)\\
&+ cpr(d_E\delta_e k - \delta_e kT_m\alpha - d\delta_I\pi\sigma + \mu\pi s_E\sigma))^2.
\end{aligned}$$

S_1 exists when $dp\pi\sigma > c\delta_e\alpha$, $\Omega \geq 0$,

$$\frac{d_E kp^2 T_m(\pi r\sigma - \delta_e k)}{cr\Big(\delta_e\Big(kp(d_E + T_m\alpha) - c\delta_I\alpha\Big) + \sigma p\pi(d_E\delta_I + \mu s_E)\Big) + \sqrt{\Omega}} > 1,$$

and

$$\frac{cr\Big(d_E\delta_e kp + p\pi\sigma(d_E\delta_I + \mu s)\Big) + d_E kp^2 T_m(\pi r\sigma + \delta_e k) + \sqrt{\Omega}}{cr\alpha(\delta_e\delta_I + d_E kpT_m)} > 1.$$

The third steady state,

$$S_2 = (T_2, I_2, V_2, e_2, E_2)$$

is the chronic infection steady state where effector cells are functional, where

$$T_2 = \frac{cr\Big(\delta_e\Big(c\delta_I\alpha + kp(T_m\alpha - d_E)\Big) - \sigma p\pi(d_E\delta_I + \mu s_E)\Big) - d_E kp^2 T_m(\delta_e k + \pi r\sigma) + \sqrt{\Omega}}{2kpr(d_E p\pi\sigma - c\delta_e\alpha)},$$

$$I_2 = \frac{c\Big(cr\Big(\delta_e(c\delta_I\alpha - kpT_m\alpha - kpd_E) - \sigma p\pi(d_E\delta_I + \mu s_E)\Big) + d_E kp^2 T_m(\pi r\sigma - \delta_e k) + \sqrt{\Omega}\Big)}{2kp(d_E p\pi\sigma - c\delta_e\alpha)(cr + kpT_m)},$$

$$V_2 = \frac{(cr\Big(\delta_e(c\delta_I\alpha - kpT_m\alpha - kpd_E) - \sigma p\pi(d_E\delta_I + \mu s_E)\Big) + d_E kp^2 T_m(\pi r\sigma - \delta_e k) + \sqrt{\Omega}}{2k(d_E p\pi\sigma - c\delta_e\alpha)(cr + kpT_m)},$$

$$e_2 = \frac{\pi\Big(cr\Big(\delta_e(c\delta_I\alpha - kpT_m\alpha - kpd_E) - \sigma p\pi(d_E\delta_I + \mu s_E)\Big) + d_E kp^2 T_m(\pi r\sigma - \delta_e k) + \sqrt{\Omega}\Big)}{2k\delta_e(d_E p\pi\sigma - c\delta_e\alpha)(cr + kpT_m)},$$

$$E_2 = \frac{cr\Big(\delta_e\Big(c\delta_I\alpha + kp(T_m\alpha + d_E)\Big) - \sigma p\pi(d_E\delta_I - \mu s_E)\Big) + d_E kp^2 T_m(\delta_e k + \pi r\sigma) - \sqrt{\Omega}}{2c\mu r(d_E p\pi\sigma - c\delta_e\alpha)}.$$

Ω is defined as before.

S_2 exists when $dp\pi\sigma > c\delta_e\alpha$, $\Omega \geq 0$,

$$\frac{d_E kp^2 T_m(\pi r\sigma - \delta_e k) + \sqrt{\Omega}}{cr\Big(\delta_e\Big(kp(d_E + T_m\alpha) - c\delta_I\alpha\Big) + \sigma p\pi(d_E\delta_I + \mu s_E)\Big)} > 1,$$

and

$$\frac{cr\alpha(\delta_e\delta_I + d_E kpT_m) + \sqrt{\Omega}}{cr\Big(d_E\delta_e kp + p\pi\sigma(d_E\delta_I + \mu s_E)\Big) + d_E kp^2 T_m(\pi r\sigma + \delta_e k)} > 1.$$

3.3.2 Jacobian

We want to study the local stability of our system (3.6-3.10). The Jacobian for this system is the same as for the previous system.

$$J = \begin{pmatrix} r(1-\frac{T+I}{T_m}) - \frac{rT}{T_m} - kV - \lambda & \frac{-rt}{T_m} & -kT & 0 & 0 \\ kV & -\delta_I - \mu E - \lambda & kT & 0 & I\mu \\ 0 & p & -c-\lambda & 0 & 0 \\ 0 & 0 & \pi & -\delta_e - \lambda & 0 \\ 0 & \frac{\alpha E}{1+e\sigma} & 0 & \frac{-\alpha EI\sigma}{(1+e\sigma)^2} & \frac{\alpha I}{1+e\sigma} - d_E - \lambda \end{pmatrix}$$

Proposition 1 The steady state S_0 is locally asymptoically stable when

$$R_{02} = \frac{kpT_m}{\delta_I + \mu\frac{s_E}{d_E}} < 1$$

and unstable otherwise.

Proof The characteristic equation for S_0 is:

$$(-d-\lambda)(-\delta_e-\lambda)(-r-\lambda)(\lambda^2 + (\delta_I + c)\lambda + (c\delta_I - kpT_m + \frac{c\mu s_E}{d_E})) = 0$$

and the corresponding eigenvalues are

$$\begin{aligned} \lambda_1 &= -\delta_E < 0, \\ \lambda_2 &= -d_E < 0, \\ \lambda_3 &= -r < 0, \\ \lambda_4 &= \frac{-cd_E - d_E\delta_I - \mu s_E + \sqrt{(cd_E + d_E\delta_I + \mu s_E)^2 - 4d(cd\delta_I + c\mu s_E - d_E kpT_m}}{2d_E}, \\ \lambda_5 &= \frac{-cd_E - d_E\delta_I - \mu s_E - \sqrt{(cd_E + d_E\delta_I + \mu s_E)^2 - 4d(cd\delta_I + c\mu s_E - d_E kpT_m}}{2d_E} < 0. \end{aligned} \tag{3.11}$$

$\lambda_4 < 0$ when $R_{02} < 1$. Therefore S_0 is locally asymptotically stable when $R_{02} < 1$.

The analytical investigation for the stablity of S_1 and S_2 is tedious and will not be presented here. All results will be numerical.

3.3.3 Numerical Analysis

As in the $s_E = 0$ case, the different steady states of system (3.6-3.10) can be reached with parameter sets in which only σ changes. σ represents the effect of a change in the rate at

which HBeAg limits the expansion of the effector cells. Figure 3.4 shows the system reaching steady state S_1 which occurs when σ is high ($\sigma = 21$ cells per mL $\times$ day.) so the immune system does not expand in the presence of HBV (E goes to zero). That leads a low steady state value for the target cells and a high steady state value for the infected cells. When $\sigma = 21$, $T_1 = 7.49 \times 10^5$ cells per mL and $I_1 = 1.03 \times 10^7$ cells per mL. For a low value of σ ($\sigma = 0.021$ cells per mL $\times$ day.) the immune system can recognize the presence of HBV and therefore create the needed effector cells, the state which steady state S_2 represents. Figure 3.5 shows the system reaching steady state S_2 with $\sigma = 0.021$. The new steady state values become $T_2 = 2.55 \times 10^6$ cells per mL, a 235.9% difference, and $I_2 = 8.89 \times 10^6$, a 13.7% difference.

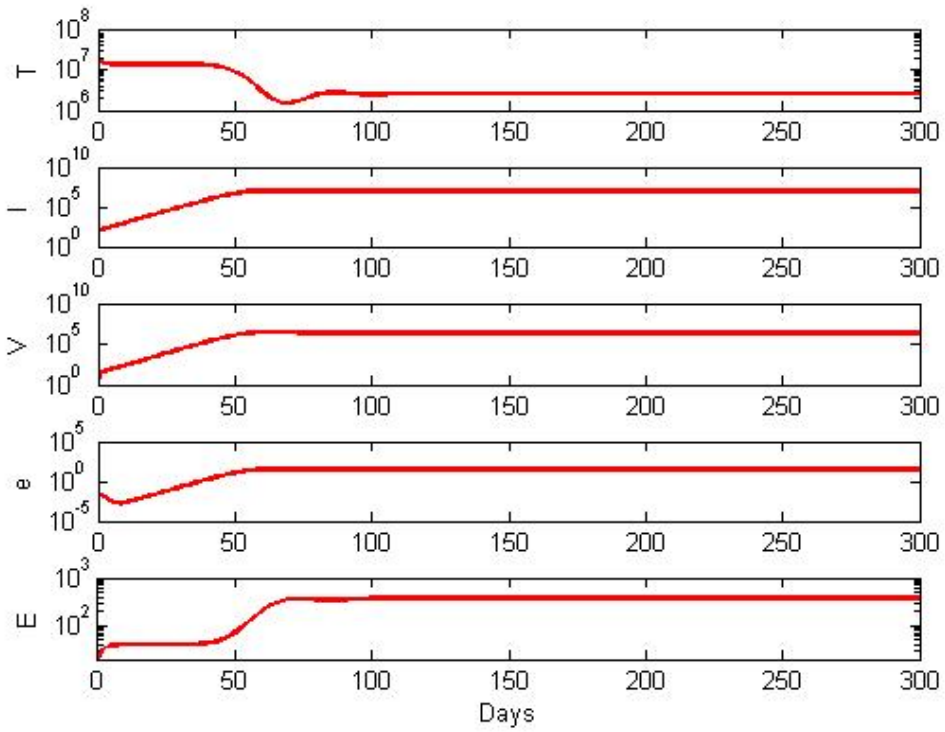

Figure 3.4: The plot of all five variables over time reaching steady state S_1 with $\sigma = 0.021$ and $s_E = 20$ cells per mL $\times$ day.

3.4 Drug Therapy

In order to model the HBV infection during drug therapy, we modified systems (3.1-3.5) and (3.6-3.10) by multiplying the infection rate, k, by $(1 - \epsilon)$ and the production rate of virions, p, by $(1 - \eta)$ where ϵ and η are the effectiveness of the drug therapy for each of those

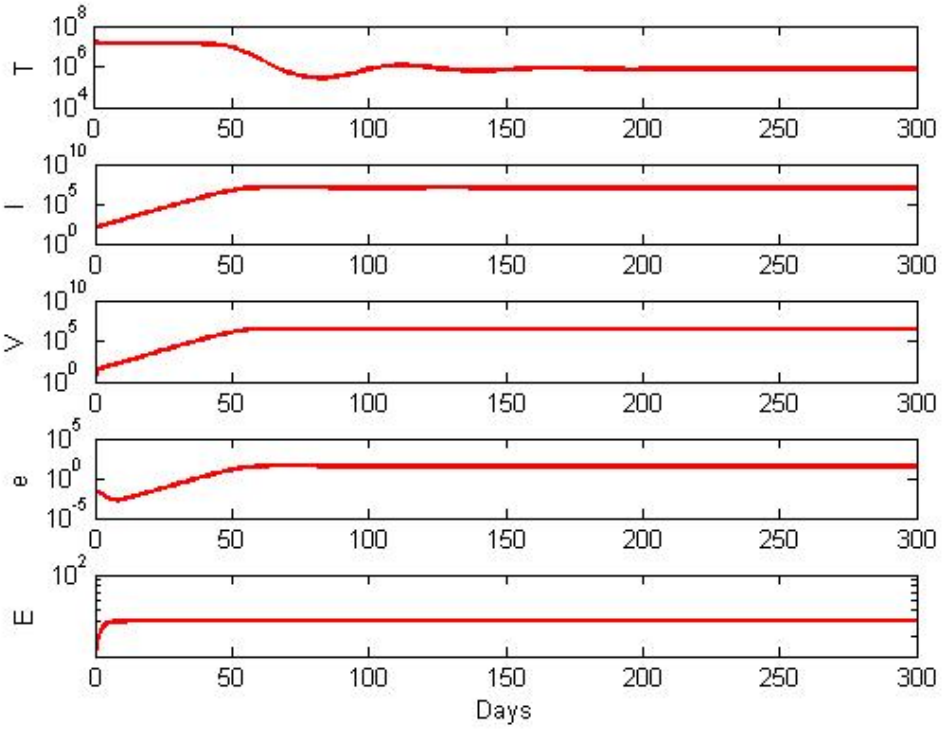

Figure 3.5: The plot of all five variables over time reaching steady state S_2 with $\sigma = 21.$ and $s_E = 20$ cells per mL $\times$ day..

biological processes, as in Lewin et. al [17]. The equations with drug therapy are:

$$\frac{dT}{dt} = rT\left(1 - \frac{T+I}{T_m}\right) - (1-\epsilon)kTV, \tag{3.12}$$

$$\frac{dI}{dt} = (1-\epsilon)kTV - \delta_I I - \mu IE, \tag{3.13}$$

$$\frac{dV}{dt} = (1-\eta)pI - cV, \tag{3.14}$$

$$\frac{de}{dt} = \pi V - \delta_e e, \tag{3.15}$$

$$\frac{dE}{dt} = \frac{\alpha IE}{1+\sigma e} - d_E E. \tag{3.16}$$

For the equations used with data fitting, we again add s_E to equation (3.16).

For the equations with drug therapy, $R_0^{new} = (1-\eta)(1-\epsilon)R_0^{old}$. $R_0^{new} < 1$ implies

that the infection free steady state will be locally asymptotically stable. For $\epsilon = 0.9$ and $\eta = 0.5$, R_0^{old} can be reduced to below one for $R_0^{old} < 20$. An estimate of $\epsilon = 0.9$ is rather low and if increased to 0.99 which is closer to estimates by other researchers [17, 25], R_0^{old} values as great as 200 can be reduced to below the critical value of one for the infection free steady state. The value of R_0^{old} is a approximately equal to 18 for the typical parameter values used to create the figures in this section, hence $\epsilon = 0.9$ and $\eta = 0.5$ would be sufficient for R_0^{new} to be less than one.

3.5 Data Fitting

3.5.1 Patient Data

We have virus level data from nine patients who were infected at birth with hepatitis B virus [18]. All patients are positive for HBeAg [18]. The data was collected twenty-six to fifty-five years following infection when they started to get immune activation and liver damage [18]. They were given drugs and were measured for four to twelve years (average 7.78 years and standard deviation of 2.2 years) [18]. The patients average age is 38.56 years with a standard deviation of 10.41 years [18]. The patients fell into four main categories based on when during the data collection they were receiving drug therapy. The four main catagories are:

1. therapy then no therapy (patients 2,3, and 6)
2. therapy only (patients 4,5, and 8)
3. two sets of therapy (patients 7 and 9)
4. no therapy then therapy (patient 1)

3.5.2 Method

Data fitting was performed in Matlab using the built-in Matlab function fminsearch. Virus curves given by the solutions of (3.6-3.10) were fitted to the no therapy patient data, while virus curves given by the solutions of (3.12-3.16) were fitted to therapy patient data. The parameters fit were α, η, and c. V_0 varied for individual patients and was set at the inital data point. The rest of the parameters were kept constant at known values (see Table 3.1) [4, 8].

3.5.3 No Therapy then Therapy

The best parameter estimates are given in Table 3.2 and the corresponding virus loads are presented in Figure 3.6. We see a variation in the viral parameter c among the patients. The drug efficacy, however, is high, with an average of 0.997 as reported previously [8, 17, 23].

Table 3.1: **Set Parameter Values**

Parameter	*Descripton*	*Value*
T_0	inital target cell value	7×10^6 cells/mL
I_0	inital infected cell value	7×10^6 cells/mL
e_0	inital HBeAg value	10 per mL
E_0	inital effector cell value	20 cells/mL
r	production rate of target cells	1 day^{-1}
T_m	carry capacity of target cells	1.36×10^7 cells/mL
k	contact rate between target cells and virus	1×10^{-10} mL/(day $\times$ virion)
μ	contact rate of I and E	1×10^{-4}day^{-1}
p	number of virions produced by an infected cell	10 virions/(day $\times$ day)
π	rate at which HBeAg is produced	5.9×10^{-8} day^{-1}
δ_e	death rate of HBeAg	0.3 day^{-1}
σ	HBeAg effect on effector cells	10 virions/(day $\times$ day)
d_E	death rate of effector cells	0.5 day^{-1}
d_I	death rate of infected cells	0.0 or 0.01 day^{-1}
ϵ	drug efficacy	0.5
s_E	Effector cell source	1 cells/day

Table 3.2: **Fitted Parameter Values**

Patient	α	η	c	ssq
2	6.84×10^{-7}	0.9995	0.51	3.85
3	1.15×10^{-6}	0.9954	7.99	4.01
6	6.68×10^{-6}	0.9962	9.49	4.79
average	2.84×10^{-6}	0.997	4.43	4.22
standard deviation	2.72×10^{-6}	1.8×10^{-3}	3.06	0.41

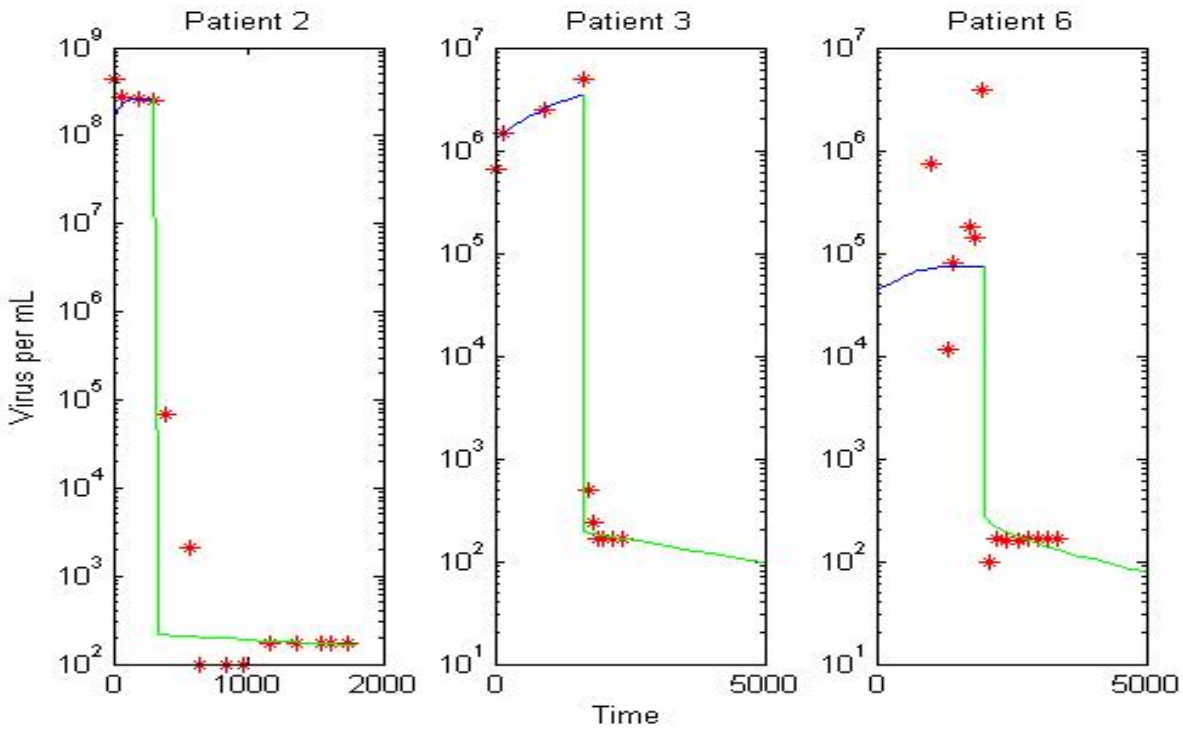

Figure 3.6: The best fit plots of Patients 2,3, and 6 who were the individuals who recieved no treatement during the first phase of data collection and then recieved therapy during the second half.

We plotted all variables to observe trends and analyze the effects of HBeAg loss. The plots for the three patients are presented in Figures 3.7, 3.8, and 3.9.

Patient 2 has the most pronounced target cell re-bound. Patients 2 and 3 exhibit similar peaks in effector cell levels of 10^4 cells per mL which arise at the beginning of therapy which correspond to a drop in infected cells, virus, and HBeAg levels and an increase in target cells. The effector cells for patient 6 are elevated even before the start of therapy. This is due to a high activation rate α as well as a high virus clearance c. We note that this patient had the lowest virus level before the start of therpay, therefore, the HBeAg was low as well. By contrast, patient 2, had the highest virus load before the start of therapy and the lowest predicted virus clearence c.

The goal of our study was to predict the moment the HBeAg is lost and, if possible, correlate it to the moment when HBeAb appears in the patients according to the patient data.

Since our variables are measured in concentration per mL, one HBeAg in the body corresponds to 3×10^{-4} HBeAg per mL, since we consider the variables are distributed in 3 L of blood. The predicted moment in which HBeAg is lost and the data showing the moment when HBeAb is first measured are shown in Table 3.3. The model provides a fairly

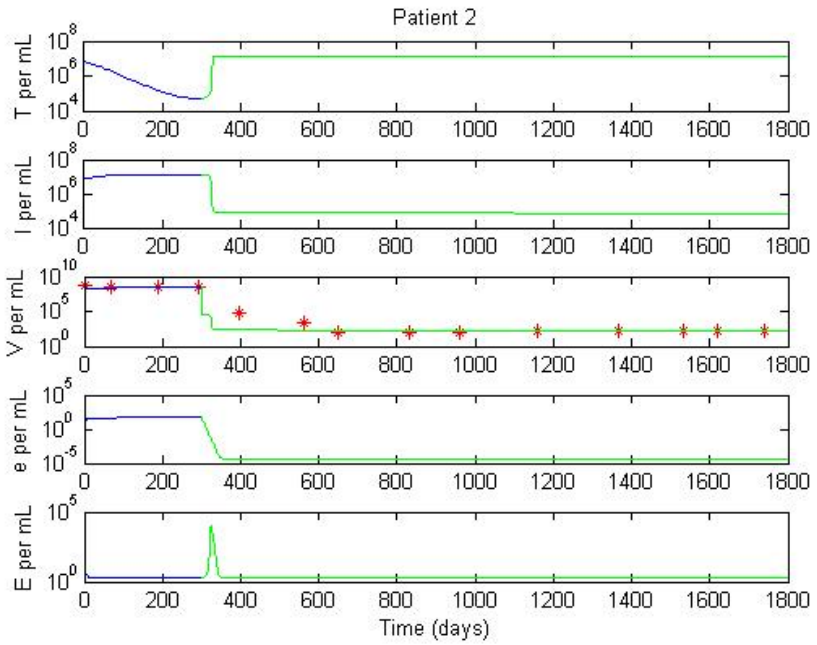

Figure 3.7: The best fit plot for Patient 2 showing all five variables.

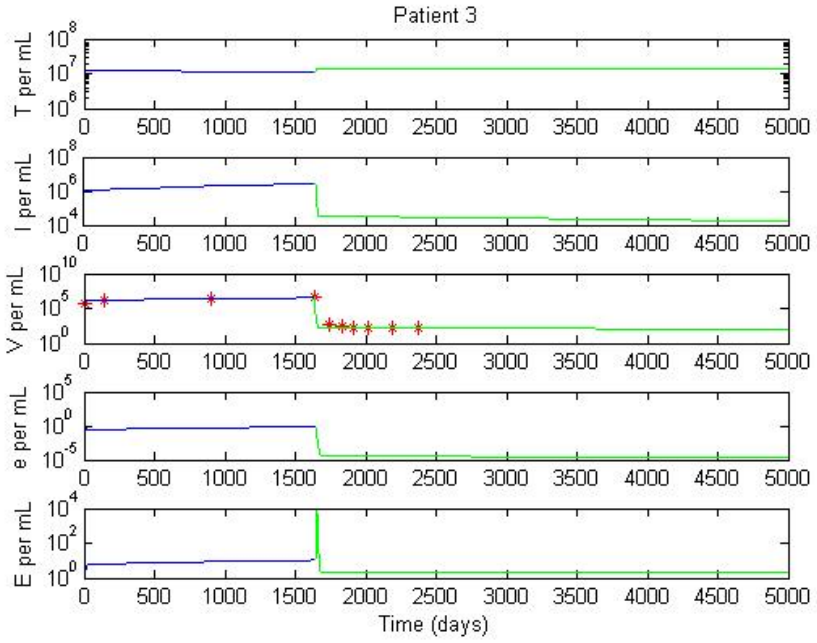

Figure 3.8: The best fit plot for Patient 3 showing all five variables.

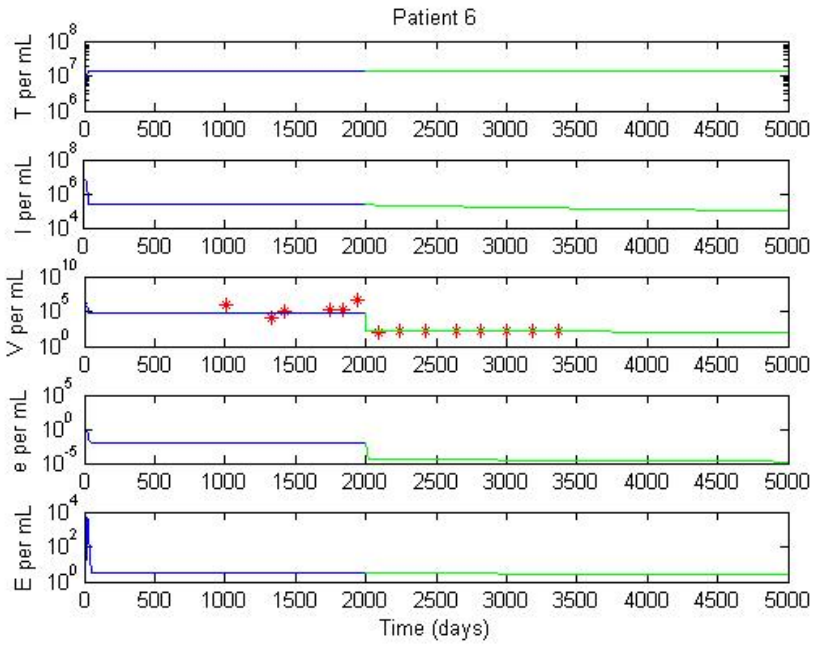

Figure 3.9: The best fit plot for Patient 6 showing all five variables.

Table 3.3: **Seroconversion Times**

Patient	Known Time	Predicted Time
2	1159.9	346
3	1742.9	1670
6	1000	2015

close estimate for the time of HBeAg loss for patient 3. However, the estimate is about one third the actual time of HBeAg loss for patient 2 and the estimate is double the known time for HBeAg loss for patient 6. The differences seen in the timing of HBeAg loss and HBeAb appearance may be due to the fact that the HBeAg is complexed to HBeAb and the complexes are not measured by the biological assays.

3.5.4 Therapy Only

The model given by system (3.12-3.16) cannot fit the data in patients 4,5, and 8 which start therapy right away. System (3.12-3.16) predicts a linear decay in the virus load. We modified the model to include a more rapid HBeAg loss, compared to the virus loss. The new model

Table 3.4: **Fitted Parameter Values**

Patient	α	μ	η	c	ssq
4	6.38×10^{-7}	3.3×10^{-3}	0.95	2.66	2.72
5	3.68×10^{-7}	1.06×10^{-4}	0.83	2.55	4.34
8	6.61×10^{-7}	3.88×10^{-5}	0.83	1.79	2.01
average	6.50×10^{-7}	1.1×10^{-3}	0.87	2.34	3.06
standard deviation	1.14×10^{-7}	1.5×10^{-3}	0.054	0.39	1.03

is:

$$\frac{dT}{dt} = rT\left(1 - \frac{T+I}{T_m}\right) - (1-\epsilon)kTV, \tag{3.17}$$

$$\frac{dI}{dt} = (1-\epsilon)kTV - \delta_I I - \mu IE, \tag{3.18}$$

$$\frac{dV}{dt} = (1-\eta)pI - cV, \tag{3.19}$$

$$\frac{de}{dt} = \pi V - \delta_e e, \tag{3.20}$$

$$\frac{dE}{dt} = \frac{\alpha IE}{1 + \sigma \exp(\nu(\tau - t))e} - d_E E. \tag{3.21}$$

We plotted models (3.12-3.16) and (3.17-3.21) together to show the differences caused by the modification. In particular, the surge of effector cells occurs corresponding at time $t = \tau$. There is a delay in the drop of the levels of the virus, infected cells and e-Antigen corresponding to the effector cell peak. Also, once the effector cells reach their highest level, the target cells begin to increase as the other populations are decreasing.

Changes in ν produce little effect in the system and a plot of the system for $\nu = 1, 5, 10$ shows the plots overlapping. Therefore we fix it at $\nu = 3$ for the data fitting.

We fit system (3.17-3.21) to the patient data for parameters α, η, c, and μ. The delay term τ was allowed to vary between patients so $\tau = 150$ for patients 4 and 5 and $\tau = 200$ for patient 8. The fixed parameter p also had to be modified so that $p = 100$ for patients 4,5, and 8. The best parameter estimates are given in Table 3.4 and the corresponding virus loads are presented in Figure 3.12. We observe a variation in the parameter μ among the patients. The drug efficacy is high with an average of 0.87, which though a 12.7% decrease from the drug efficacy for patients 2, 3, and 6, is still within a range previously reported [8, 17, 23].

We plotted all variables to observe trends and analyze the effects of HBeAg loss. The plots for the three patients are presented in Figures 3.13, 3.14, and 3.15.

All three patients show a peak in effector cell levels at time $t = \tau$. The height and width of the peak varies between the three patients and seems to be correlated with the parameter μ. Patient 4 whose effector cell levels have a peak of about 10^1 cells per mL with

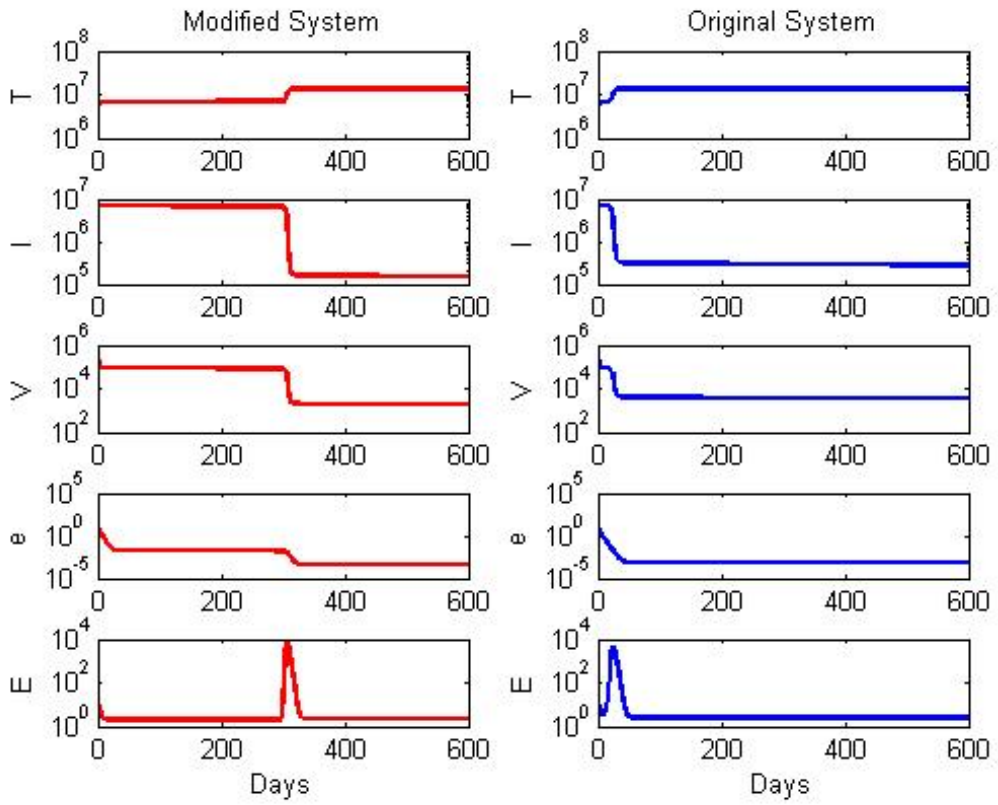

Figure 3.10: System (3.12-3.16) appears in blue (right) and the modified System (3.17-3.21) is plotted in red (left). The peak in the effector cells occurs just after $t = \tau = 300$.

the cells are elevated above the steady state for about 300 days, has the highest μ. Patient 8 has the lowest value for μ and the effector cell levels for patient 8 reach a peak of about 10^4 cells per mL with that peak beginning and ending in a span of about 50 days. Patient 5 whose μ value is between the μ value for patients 4 and 8 has an effector cell level peak value and time between that of the other two patients. The peaks of effector cell levels coincide with a more rapid drop in infected cells, virus, and HBeAg levels.

In comparison with patients 2,3, and 6, the average value for c showed a 46.9% decrease and the average value for α was also lower in patients 4,5, and 8 with a 77.1% decrease.

The predicted moment in which HBeAg is lost and the data showing the moment when HBeAg is first measured are shown in Table 3.5. The model provides an estimate that is acurate within a 4% error range of the actual data for patients 4 and 8. However, the estimate for patient 5 is about five times too large. The patient data did state that patient 5 underwent HBeAg seroconversion twice. The second seroconversion took place at time $t = 1132$, which is closer to our model's estimate, however, the model's prediction is still late.

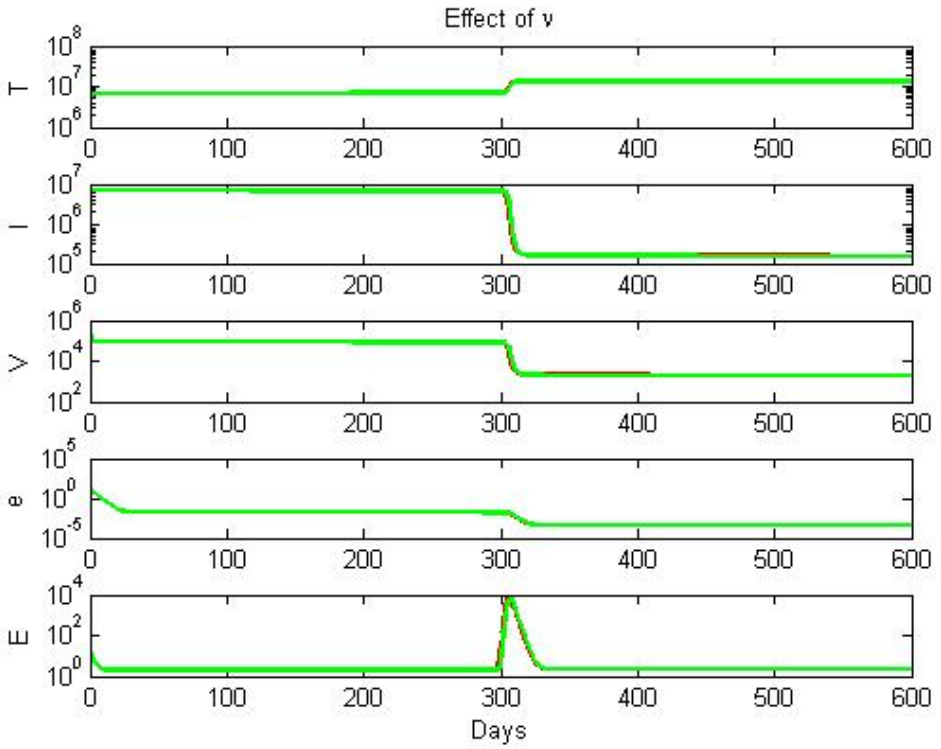

Figure 3.11: System (3.17-3.21) is plotted in blue for $\nu = 1$, red for $\nu = 5$, and green for $\nu = 10$ and for each case, $\tau = 300$.

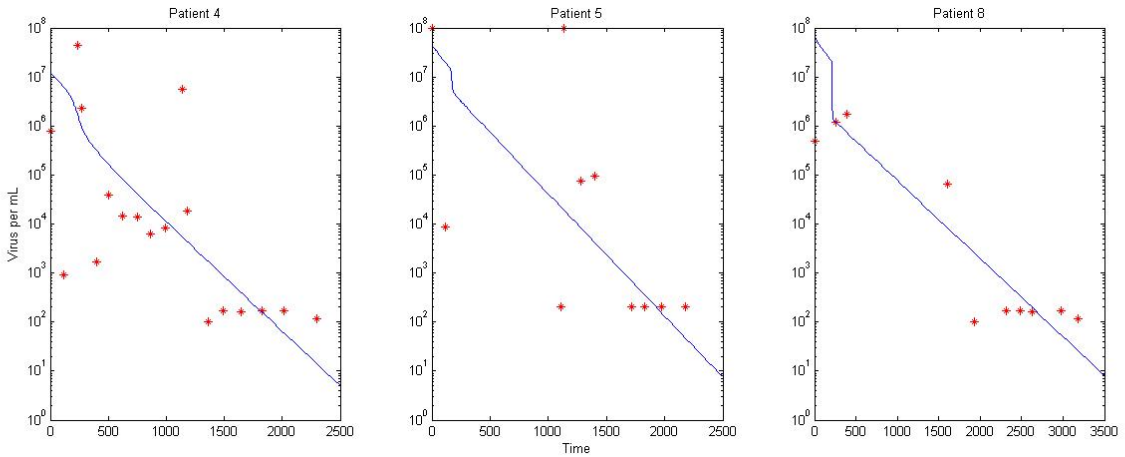

Figure 3.12: The best fit plots of Patients 4,5, and 8 who were the individuals who recieved treatement at each time step in data collection.

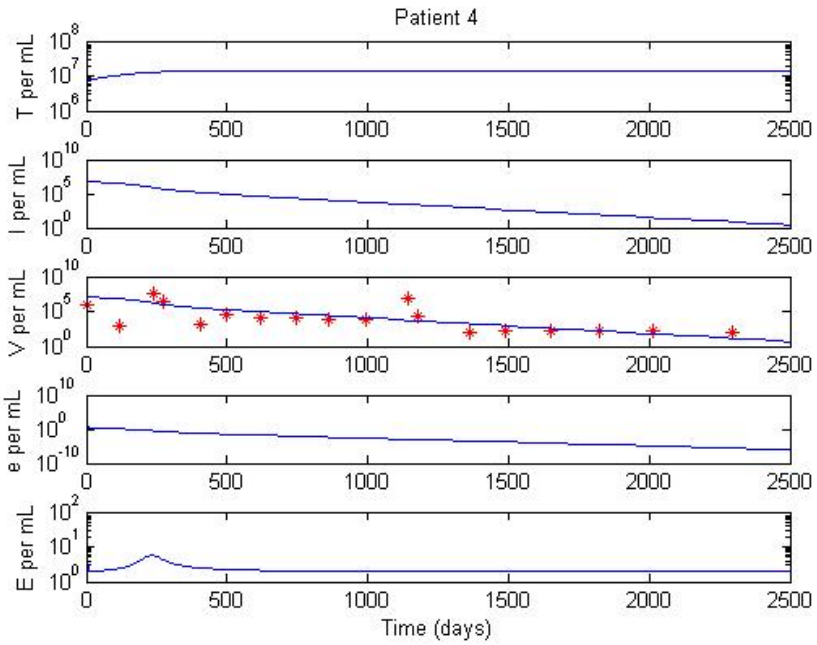

Figure 3.13: The best fit plot for Patient 4 showing all five variables.

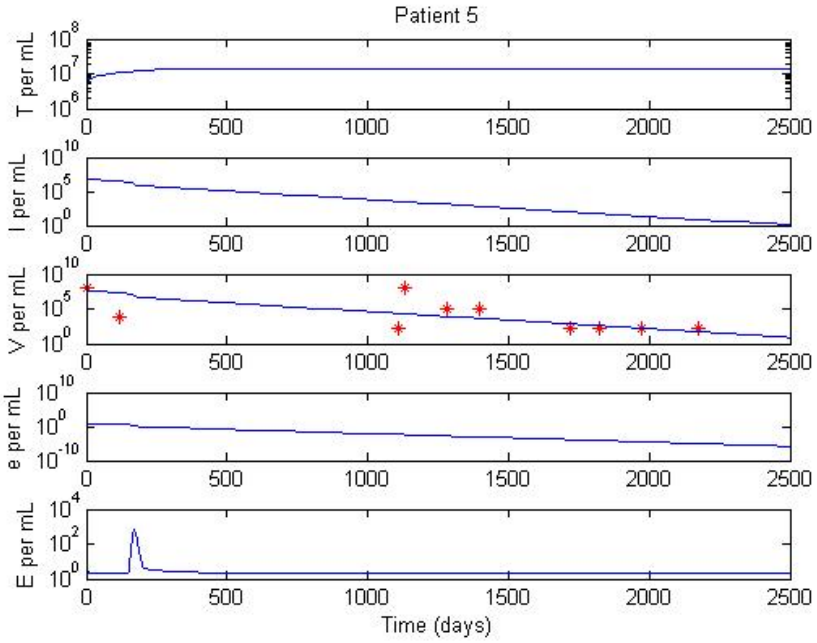

Figure 3.14: The best fit plot for Patient 5 showing all five variables.

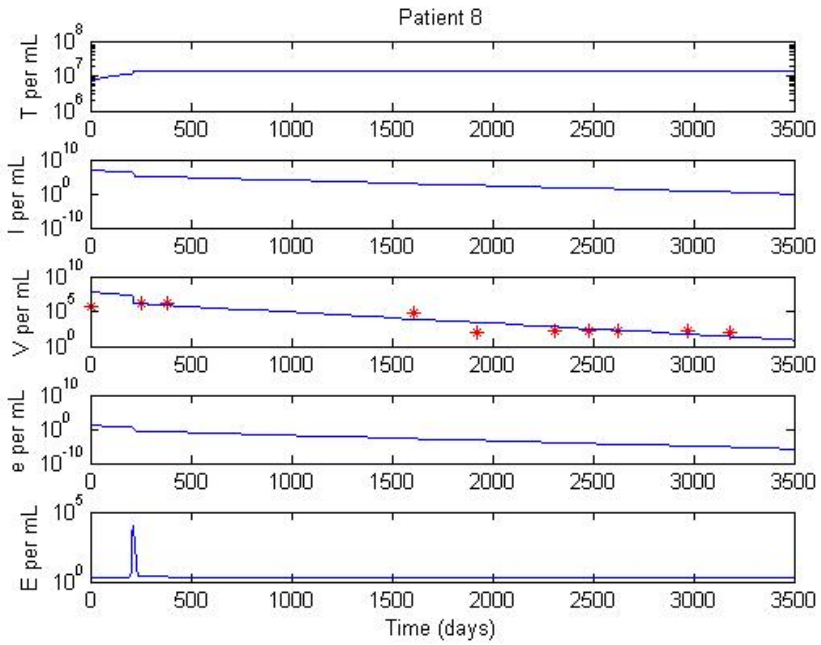

Figure 3.15: The best fit plot for Patient 8 showing all five variables.

Table 3.5: **Seroconversion Times**

Patient	Known Time	Predicted Time
4	1490.4	1505
5	332.6	1679
8	2310.7	2229

3.5.5 Two Sets of Therapy

We used systems (3.6-3.10) and (3.17-3.21) to fit the patient data for parameters α, η, c, and μ. The delay term τ was allowed to vary between patients so $\tau = 0$ for patients 7 and $\tau = 100$ for patient 9. The fixed parameter p was again modified so that $p = 10$ for patients 7 and 9. Data fitting for patient 9 required another parameter to be fit as well: η_2 which is the drug efficacy for the second set of drug therapy for patient 9. Since different drug treatments have different efficacies, the existance of η_2 can be justified biologically. Including η_2 for patient 7 did not change the ssq significantly and $\eta \approx \eta_2$ so was not included in the data fit. The best parameter estimates are given in Table 3.6 and the corresponding virus loads are presented in Figure 3.16. The ssq is high due to the complexity of adding the second therapy set. We observe a variation in the parameter α between the patients. The drug efficacy is high with an average of 0.92, which though a 7.27% decrease from the drug efficacy for patients 2, 3, and 6, is still within a range previously reported [8, 17, 23].

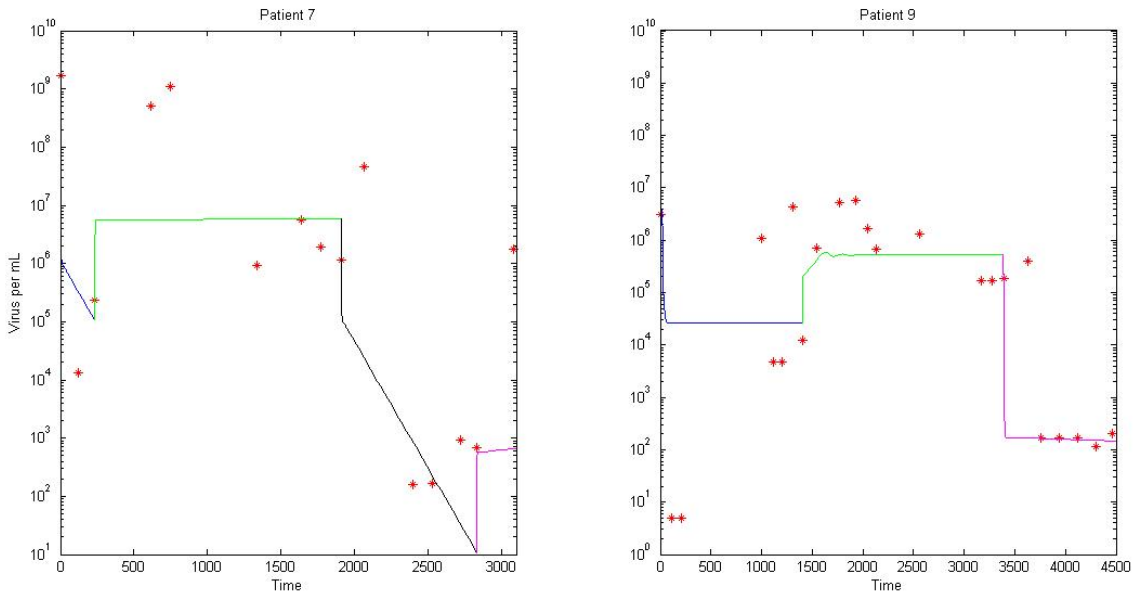

Figure 3.16: The best fit plots of Patients 7 and 9 who were the individuals where treatment was present then treatment stopped before resuming again.

Table 3.6: **Fitted Parameter Values**

Patient	α	μ	η	c	η_2	ssq
7	4.15×10^{-9}	6.09×10^{-5}	0.981	1.27		8.24
9	8.27×10^{-6}	4.74×10^{-5}	0.868	2.3049	0.998	8.50
average	4.14×10^{-5}	5.41×10^{-5}	0.9245	1.79		8.37

We plotted all variables to observe trends and analyze the effects of HBeAg loss. The plots for the three patients are presented in Figures 3.17 and 3.18.

Patient 9 experiences a sharper and lower drop during the first set of therapy than patient 7, however during the second set of therapy, patient 7 sees the greater virus level decrease. Patient 7's data also includes some data without treatment following the second set of therapy. That data indicates that once therapy stops, the virus will increase, however our model predicts that HBeAg will remain below the level of detection. The model indicates that the effector cells are a lot more active for patient 9 as compared to patient 7. Patient 9 shows peaks of approximately 10^4 cells per mL in the effector cell populations at the beginning of each set of therapy as well as an elevated level of effector cells during the period of no therapy. The effector cells in patient 7 do not show peaks at any time. The peaks in the effector cell levels of patient 9 correspond to a more rapid decrease in virus level, forcing it to a steady state faster than patient 7 where linear decays appear. HBeAg levels are lower for patient 9 than patient 7 during the first set of therapy. The difference in effector cell

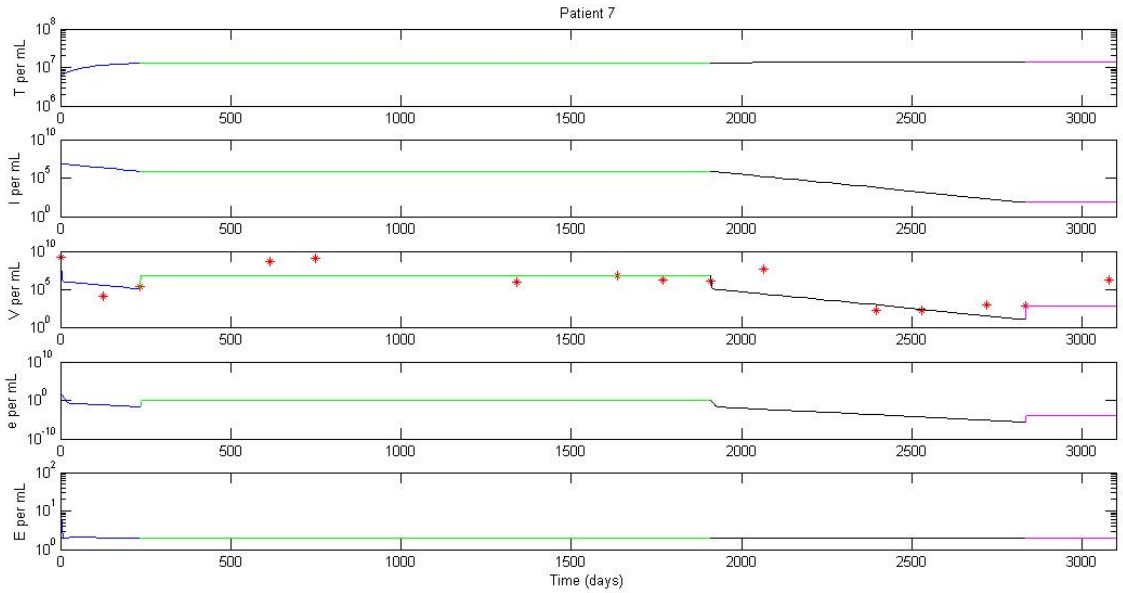

Figure 3.17: The best fit plot for Patient 7 showing all five variables.

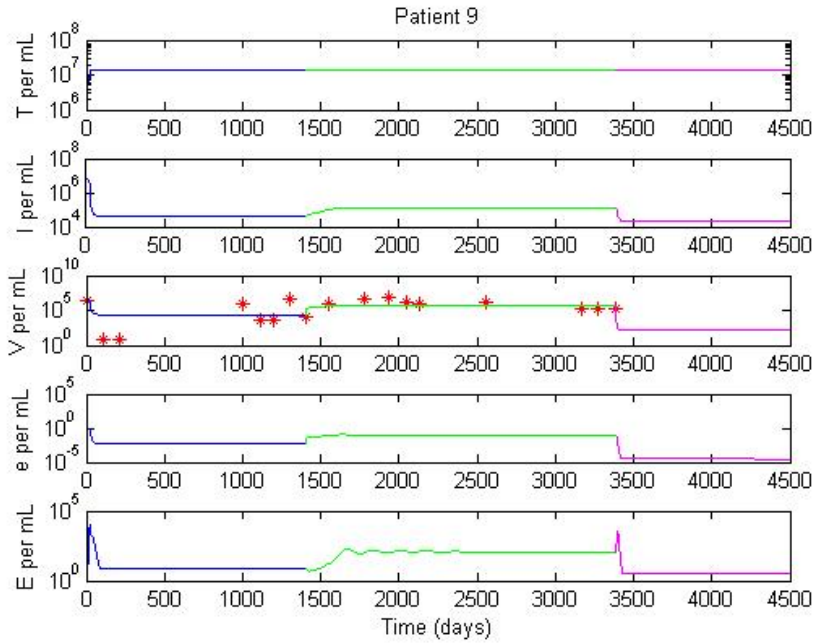

Figure 3.18: The best fit plot for Patient 9 showing all five variables.

levels may be attributed to the parameter α. α has a 99.94% decrease in patient 7 compared to patient 9.

Table 3.7: **Seroconversion Times**

Patient	Known Time	Predicted Time
7	2720	2345
9	4307	3410

The average for c for patients 7 and 9 is consistent with the average for patients 4,5, and 8, and as a 23.6% difference less than the average for patients 2,3 and 6.

The predicted moment in which HBeAg is lost and the data showing the moment when HBeAg is first measured are shown in Table 3.5. The model provides an estimate that is acurate within a 14% error range of the actual data for patients 7. However, the estimate for patient 8 is very low.

3.5.6 Therapy then No Therapy

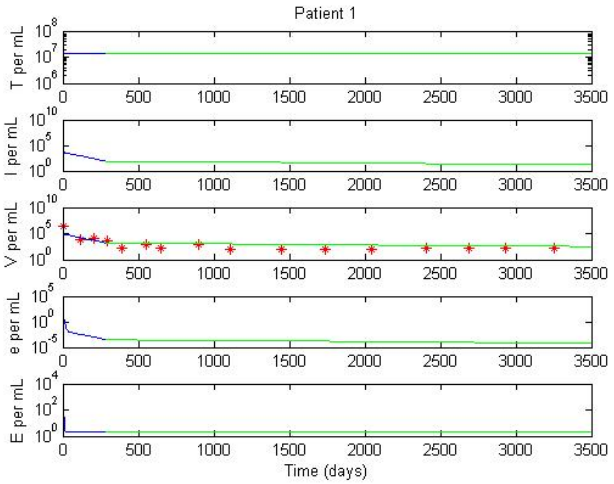

Figure 3.19: The best fit plot of Patient 1 who was the individual whose treatment stopped during data collection.

We used systems (3.6-3.10) and (3.17-3.21) to fit the patient data for parameters α, η, c, and μ. The delay term τ was set to $\tau = 0$ for patient 1. The fixed parameter p was again modified so that $p = 100$ for patients 7 and 9. The best parameter estimates are given in Table 3.8 and the corresponding virus loads are presented in Figure 3.19. We observe that ν is very low. There is a 99.98% difference between ν for patient one and the second lowest fitted ν. The drug efficacy for patient 1 is not consistant with the range previously reported [8, 17, 23].

We plotted all variables to observe trends and analyze the effects of HBeAg loss.

Table 3.8: **Fitted Parameter Values**

Patient	α	μ	η	c	ssq
1	6.96×10^{-7}	8.9×10^{-3}	1.66×10^{-4}	4.9778	1.83

The plot for patient 1 is presented in Figure 3.20.

Comparison to the data fit estimates for Patient 1 from the equations without the time delay, the time delay leads to a higher estimate for α and significantly lower estimates for η and c. The ssq and visual qualities of the fit are better, but it is not known if the increase in ssq is significant enough to justify using a more complicated model.

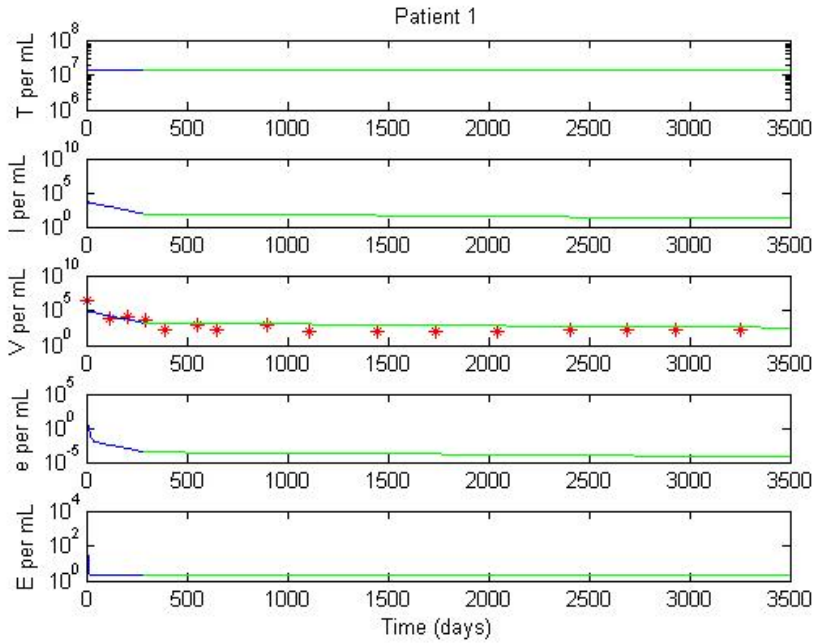

Figure 3.20: The best fit plot for Patient 1 showing all five variables.

A peak in effector cell levels of about 10^2 appears at time $t = 0$ which coincides with a drop in infected cells, virus and HBeAg levels. The parameter α is the same order of magnitude as the average for α with patients 4,5, and 8. Like patient 4, patient 1 has a value of μ that is order of magnitude 10^{-3} and is the largest μ fit observed.

The predicted moment in which HBeAg is lost and the data showing the moment when HBeAg is first measured are shown in Table 3.5. The model provides an estimate that is very low, the known time is almost double the estimate.

Table 3.9: **Seroconversion Times**

Patient	Known Time	Predicted Time
1	2042	1185

3.6 Liver Damage

The model can be used to calculate the percent of liver damage which occurs within the first 100 days after immune activation [4]. The liver damage is calculated by $a_s(\tau)$ [4] where

$$a_s(\tau) = \int_0^\tau \mu \frac{c}{p} I(t)E(t)dt.$$

A plot of the liver damage as related to drug efficacy, η is presented in Figure 3.21. Unlike previous estimates of liver damage calculated without drug therapy where maximal liver damage was 180%, the maximal liver damage with drug therapy is less than 13% which is considered minimal [4].Therefore drug therapy helps reduce liver damage during HBV infection.

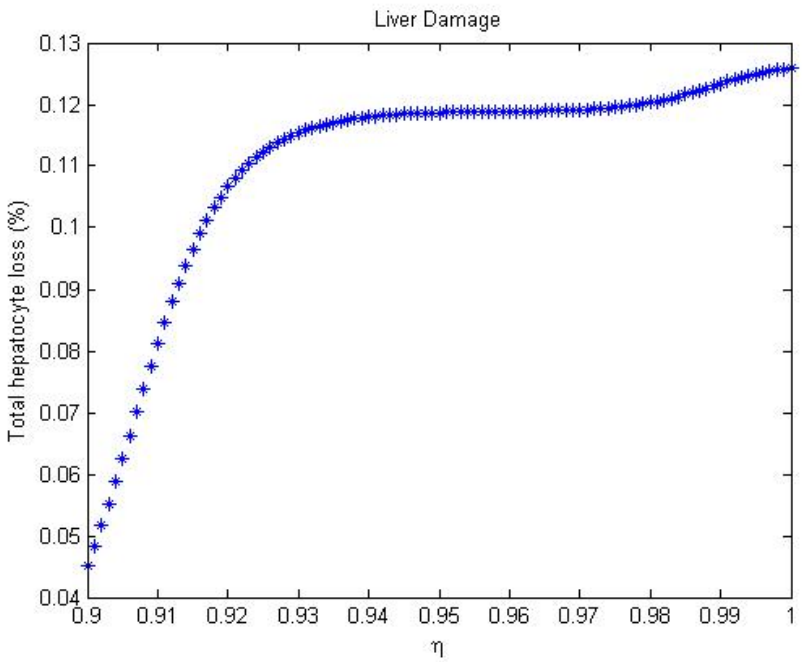

Figure 3.21: The plot of liver damage percentage which occurs during the first 100 days after immune activation compared to drug efficacy, η.

3.7 Conclusion

HBeAg plays a critical role in the pathogenesis of HBV infection. To determine whether it may be an agent in chronicity, we developed mathematical models of HBV infection in the presence of HBeAg. We derived conditions of chronic and cleared infections based on the HBeAg strength in inducing immune tolerance. Then we investigated how different patterns of drug therapy affect HBeAg loss. We see that our model predicts that HBeAg is lost earlier than the emergence of HBeAb. Another investigation is needed to determine the underlying mechanisms for the observed delay. Also, additional future work could include numerical investigations, sensitivity analysis and a globalized parameter estimation method. Such an understanding of a mathematical model of the role of e-Antigen in hepatitis B virus infection is needed since early HBeAg loss is known to lead to successful recovery from an HBV infection.

Bibliography

[1] Linda J. S. Allen. *An Introduction to Mathematical Biology*. Pearson Education, Inc., 2007.

[2] Y.C. Chen, S.F. Huang, C.M. Chu, and Y.F. Liaw. Serial hbv dna levels in patients with persistently normal transaminase over 10 years following spontaneous hbeag serconversion. *Journal of Viral Hepatitis*, 19:138–146, 2012.

[3] C.M. Chu and Y.F. Liaw. Chronic hepatitis b virus infection acquired in childhood: special emphasis on prognostic and therapeutic implication of delayed hbeag serconversion. *Journal of Viral Hepatitis*, 14:147–152, 2007.

[4] Stanca Ciupe and Sara Hews. Mathematical models of e-antigen mediated immune tolerance and activation following prenatal hbv infection. *Plos One*, 7.7:1–11, 2012.

[5] Stanca M. Ciupe, Ruy M. Ribeiro, Patrick W. Nelson, Geoffrey Dusheiko, and Alan S. Perelson. The role of cells refractory to produce infection in acute hepatitis b viral dynamics. *PNAS*, 104:5051–5055, 2007.

[6] Stanca M. Ciupe, Ruy M. Ribeiro, Patrick W. Nelson, and Alan S. Perelson. Modeling the mechanisms of acute hepatitis b virus infection. *Science Direct: Journal of Theoretical Biology*, 247:23–35, 2007.

[7] Stanca M. Ciupe, Ruy M. Ribeiro, and Alan S. Perelson. Antibody responses during hepatitis b viral infection. *PLOS Computational Biology*, 10:1–16, 2014.

[8] Harel Dahari, Emi Shudo, Ruy M Ribeiro, and Alan S Perelson. Modeling complex decay profiles of hepatitis b virus during antiviral theorapy. *Hepatology*, 49.1:32–38, 2009.

[9] Lijuan Du, Dongwei Huang, and Qizhi Xie. A mathematical model for acute hepatitis b virus infection. *IEEE*, pages 1109–1113, 2010.

[10] Nelson Fausto, Jean S. Campbell, and Kimberly J. Riehle. Liver regeneration. *Hepatology*, 43:S45–S53, 2006.

[11] Hepatitis B Foundation. Additional blood tests, March 2014.

[12] Hepatitis B Foundation. Statistics, February 2014.

[13] Luca G. Guidotti and Francis V. Chisari. Immunobiology and pathogenesis of viral hepatitis. *The Annual Review of Pathology: Mechanisms of Disease*, 1:23–61, 2006.

[14] Luca G. Guidotti, Brent Matzke, and Francis V. Chisari. Hepatitis b virus replication is cell cycle independent during liver regeneration in transgenic mice. *Journal of Virology*, 71:4804–4808, 1997.

[15] Maria-Christina Jung and Gerd R. Pape. Immuneology of hepatitis b infection. *The Lancet: Infectious Diseases*, 2:43–50, 2002.

[16] Daryl T.Y. Lau, M. Farooq Khokhar, Edward Doo, Marc G. Ghany, David Herion, Yoon Park, David E. Kleiner, Peter Schmid, Lynn D. Condreay, Josee Gauthier, Mary C. Kuhns, Jake T. Liang, and Jay H. Hoofnagle. Long-term therapy of chronic hepatitis b with lamivudine. *Hepatology*, 4:828–834, 2000.

[17] Sharon R. Lewin, Ruy M. Ribeiro, Tomos Walters, George K. Lau, Scott Bowden, Stephen Locarnini, and Alan S. Perelson. Analysis of hepatitis b viral load decline under potent therapy: Complex decay profiles observed. *Hepatology*, 34:1012–1020, 2001.

[18] MH Malespin, EK Kemerly, BJ Luc, PS Mettu, JL Thomas, SS Wong, SJ Cotler, and H. Dahari. Longitudinal analysis of hbv replication and alt levels in an urban chinatown community. *University of Illinois at Chicago, College of Medicine - Research Forum*, 2011.

[19] Mayo Medical Laboratories Mayo Clinic. Interpretive handbook: Test 8311: Hepatitis be antigne and hepatitis be antibody serum.

[20] Avidan U. Neumann, Nancy P. Lam, Harel Dahari, David R. Gretch, Thelma E. Wiley, Thomas J. Layden, and Perelson Alan S. Viral dynamics in hepatitis b virus infection. *Science*, 282:103–107, 1998.

[21] Martin A. Nowak, Sebastian Bonhoeffer, Andrew M. Hill, Richard Boehme, Howard C. Thomas, and Hugh McDade. Viral dynamics in hepatitis b virus infection. *PNAS*, 93:4398–4402, 1996.

[22] V. Periwal, J.R. Gaillard, L. Needleman, and C. Doria. Mathematical model of liver regeneration in human live donors. *Journal of Cellular Physiology*, 229:599–606, 2013.

[23] Ruy M. Ribeiro, Georgios Germanidis, Kimberly A. Powers, Bertrand Pellegrin, Paul Nikolaidis, Alan S. Perelson, and Jean-Michel Pawlotsky. Hepatitis b virus kinetics under antiviral therapy sheds light on differences in hepatitis b e antigen positive and negative infections. *Journal of Infectious Diseases*, 202:1309–1318, 2010.

[24] Christoph Seeger and William S. Mason. Hepatitis b virus biology. *American Society for Microbiology*, 64:51–68, 2000.

[25] Manuel Tsiang, James F. Rooney, John J. Toole, and Graig S. Gibbs. Biphasic clearance kinetics of hepatitis b virus from patients during adefovir dipivoxil therapy. *Hepatology*, 29:1863–1869, 1999.

[26] Renae Walsh and Stephen Locarnini. Hepatitis b precore protein: Pathogenic potential and therapeutic promise. *Yonsei Med J*, 53:875–885, 2012.

[27] WHO. Hepatitis b, March 2015.

[28] G.Q. Witten and A.S. Perelson. Modelling the cellular-level interaction between the immune system and hiv. *South African Journal of Science*, 100:1–5, 2004.

[29] Shuang Wu, Fumio Imazeki, Fuat Kurbanov, Kenichi Fukai, Makoto Arai, Tatsuo Kanda, Yutaka Yonemitsu, Yasuhito Tanaka, Masashi Mizokami, and Osamu Yokosuka. Evolution of hepatitis b genotype c viral quasi-species during hepatitis b e antigen seroconversion. *Journal of Hepatology*, 54:19–25, 2011.

[30] Jing Zhang, Wei-Jia Xu, Qing Wang, Yong Zhang, and Ming Shi. Prevalence of the precore g1896a mutation in chinese patients with e-antigen negative hepatitis b virus infection and its relationship to pre-s1 antigen. *Brazilian Journal of Microbiology*, 40:965–971, 2009.